

Finite Element Simulation of Electrorheological Fluids

by
Chanryeol Rhyou

Submitted to the Department of Mechanical Engineering
in partial fulfillment of the requirements for the degree of
Master of Science in Mechanical Engineering
at the

MASSACHUSETTS INSTITUTE OF TECHNOLOGY

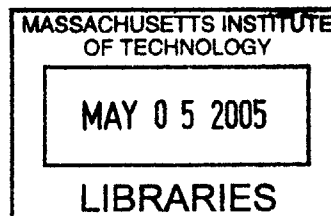
February 2005

© Massachusetts Institute of Technology 2004. All right reserved.

Author
Department of Mechanical Engineering
October 15, 2004

Certified by
Neville Hogan
Professor, Mechanical Engineering; Brain & Cognitive Sciences
Thesis Supervisor

Accepted by
Lallit Anand
Chairman, Department Committee on Graduate Students



BARKER

Finite Element Simulation of Electrorheological Fluids

by
Chanryeol Rhyou

Submitted to the Department of Mechanical Engineering
On October 15, 2004, in partial fulfillment of the
Requirements for the degree of
Master of Science in Mechanical Engineering

Abstract

Electrorheological (ER) fluids change their flow properties dramatically when an electric field is applied. These fluids are usually composed of dispersions of polarizable particles in an insulating base fluid or composed of liquid crystal polymer. To build more suitable and complicated designs for application of ER fluid, the simulation of ER fluid as well as experiments are important. First, fundamental fluid motions of Newtonian fluids are simulated and checked by comparing them with mathematical calculation. Second, among many models of ER fluid, the Bingham plastic fluid was chosen to represent the ER fluidic behavior in case of the heterogeneous ER fluid. Also, shear stress-strain rate relation of ER fluid was simulated in case of shear modes and pressure modes in both fluids; heterogeneous and homogeneous fluid. Also, the simulated shear strain-stress relationship was compared with experimental results.

Thesis Supervisor: Neville Hogan

Title: Professor, Mechanical Engineering; Brain & Cognitive Science

Acknowledgments

Above all, I would like to thank Professor Neville Hogan for his careful advice for the past 2 years. His guidance gave me good intuition and large insight through my research work and made me solve my research problems. Also I thank to the Principal research scientist of our group, Dr. Igo Krebs for his careful teaching and consideration. His acrid questions in our group meeting helped me to understand my research situation and make me choose the right way.

I owed a lot of things to not only my old research group members, Steve, Jerry, Laura, Sue but also my ex-lab members, Miranda, James, Jason and Mike. They always greeted and helped me, whenever and whatever I asked them. Especially I would like to thanks my two ISN lab mates, Doug and Tom. It was my pleasure to work with them. I couldn't finish my thesis without Tom's valuable advice, Doug's collaboration and solving our research problem together. When I began my project with them, I had to start from almost nothing because this is the totally new project and we didn't have much information related with my project. To gather the full information, we started from the literature review and we always shared our information and discussed our problems and goals.

How can I forget our new group members, Steven, Sarah, Shelly? During writing my thesis, Steven always encouraged me to concentrate on my work. And Dr. Hong and Thomas, who were members of Prof. Bathe's group, always gave me the technical expertise in using ADINA and encouraged me to think of the breakthrough of my research problem. Moreover, with my heart, I thank my parents and my family for their entire support, which made me work in the U.S and inspired me to the future efforts. Finally, I would like to thank Adlar J. Kim, Jeongik Lee, Shinwoo Kang, Jaejeen Choi, Insuk Choi, Jennifer Shin, Daekeun Kim , Taesik Lee and his family and any other MIT friends.

This work was supported by the Institute for Solider Nanotechnology

Contents

Ch1. Introduction	13
1.1 ISN Project	13
1.2 Team 4 Project	14
1.3 Thesis overview	16
Ch2. Electrorheological Fluid	16
2.1 Historical backgrounds and definition	16
2.1.1 History	16
2.1.2 Definition and applications	17
2.2 Classification of ER fluid	19
2.2.1 Functional classification	19
2.2.2 Particle-based classification	20
2.2.3 Gigantic ER fluid	22
2.3 Mechanisms and Properties of ER fluid	23
2.3.1 Heterogeneous ER fluids	24
2.3.2 Homogeneous ER fluids	25
2.4 Magnetorheological fluid	28
.....		
Ch3. Finite Element Method	29
3.1 Finite Element Method	29

3.1.1 Finite element method ...	29
3.1.2 Galerkin method	32
3.2 ADINA	35
.....	
Ch4. Mathematical modeling and FEM simulation	37
4.1 Mathematical modeling of the ER fluid	37
4.1.1 Bingham plastic fluid and Newtonian fluid	37
4.1.2 Three basic motions of ER fluid applications	39
4.1.3 Other fluid modeling	45
4.2 Parameters of Bingham plastic	46
4.3 FEM simulations	48
4.3.1 The overview of experimental settings	48
4.3.2 FEM modeling	50
4.3.3 Modeling of each simulation	53
.....	
Ch5. Results and conclusion	59
5.1 Results and discussion	59
5.2 Conclusion	83
5.3 Future work	83

List of Figures

Fig 2.1 - Overview of the polishing using ER fluid [29]	18
Fig 2.2 - Fig 2.3 Gigantic ER fluid – image of particles (left) and static yield stress vs. electric field (right) [8].	23
Fig 2.3 - The mechanisms of two different ER fluids	23
Fig 2.4 – Electropolarization	24
Fig 2.5 – Stress-shear strain rate relationship of two different types	26
Fig 2.6 – Three different Miesowicz viscosities of LCP	27
Fig 2.7 - The reorientation of LCP by the electric field	27
Fig 4.1 – The relationship of Newtonian and non Newtonian fluids between shear stress and shear rate	37
Fig 4.2 – Three basic flow modes	39
Fig 4.3 – the flow in y-z direction	41
Fig 4.4 - The extended Bingham model and the forced velocity characteristic for the extended Bingham model from [41]	46
Fig 4.5 – Three element model from [41]	46
Fig 4.6 - Dimensionless stress result from the electrostatic polarization	48
Fig 4.7 - The theoretical prediction of the yield stress of our ER fluid	49
Fig 4.8 - Overview of the experimental setting	50
Fig 4.9 - Dimension of the simulation modeling	51
Fig 4.10 - Illustration of FEM boundary conditions	52
Fig 4.11 - Three different side boundary conditions	53

Fig 4.12 - Three different region of the Bingham material	54
Fig 4.13 - The boundary conditions of simple shear mode	56
Fig 4.14 - External velocity profile	56
Fig 4.15 - Boundary conditions in the pressure mode	56
Fig 4.16 - The external velocity profile and the boundary conditions on the inclined plate	57
Fig 4.17 - The external velocity profile and the boundary conditions with pressure gradient	58
Fig 4.18 - The boundary conditions in the squeeze mode	58
Fig 5.1 - y-velocity profile at 2mm/s	59
Fig 5.2 - The pressure difference and shear stress at 2mm/s	60
Fig 5.3 - y-velocity and shear stress at 2mm/s in case of Homogeneous ER fluid at 1.3V	61
Fig 5.4 - y-velocity profile at 0s, 0.1s, 0.2s with the increasing velocity up to 2mm/s	62
Fig 5.5 - pressure distribution with the increasing velocity up to 2mm/s	62
Fig 5.6 - shear stress distribution with the increasing velocity up to 2mm/s	63
Fig 5.7- Velocity vs. shear stress of heterogeneous ER fluid (0, 1, 2, 3, 4 kV/mm) and homogenous ER fluid (0, 1, 2, 3 kV/mm)	64
Fig 5.8 - The pressure gradient, y-velocity profile and shear stress in the case of homogeneous ER fluid at 2kV/mm	65
Fig 5.9 - The pressure and shear stress of the solid region of Bingham plastic fluid the plastic at 0.1sec, 3kV/mm	66
Fig 5.10 - The pressure and shear stress of the solid region of Bingham plastic fluid the plastic at 0.2sec, 3kV/mm	66
Fig 5.11 - The external velocity profile for the shear mode with inclined plate	67

Fig 5.12 - y- velocity profile in the inclined plate when the times are 1,2,3,4,5 and 15 sec at 1kV/mm	69
Fig 5.13 - y- velocity profiles in the three sections	69
Fig 5.14 – The pressure gradient when times are 1,2,3,4,5 and 15 sec at 1kV/mm	71
Fig 5.15 - yz stress when times are 3, 4, 5 and 15 sec at 1kV/mm	71
Fig 5.16 - shear stress when it has two different viscosities: 30.9 and 29.4 (Pa•s)	72
Fig 5.17 – The boundary conditions when the viscosities of elements are different: Each element has its own viscosity and 10 elements compose the whole structure	72
Fig 5.18 – Pressure gradient and shear stress at 2kV/mm	73
Fig 5.19 - y-velocity distribution and profile at 2kV/mm	73
Fig 5.20 - Shear stress at 2kV/mm when it has a constant viscosity and a variable viscosity	74
Fig 5.21 - The external velocity condition for the shear mode with inclined plate and the flow velocity profile	75
Fig 5.22 - The velocity profiles at four different pressure gradients	76
Fig 5.23 - The velocity profiles of heterogeneous ER fluid when pressure gradients is – 500 (Pa/ μ m)	76
Fig 5.24 - The shear stress distribution when the pressure is 12000 Pa	77
Fig 5.25 - Shear stress distribution when the height is 9 μ m	77
Fig 5.26 - The pressure and shear stress distribution in the squeeze mode when the external pressure was increased by 1000Pa/s	78
Fig 5.27 – Y and z displacements when the pressure was 4000 Pa	79
Fig 5.28 – The internal pressure and shear stress distribution when the displacement was -0.25, -0.5, -75(μ m)	80
Fig 5.29 – The internal pressure and shear stress distribution when the displacement was -1 (μ m) : the shear stress was symmetric	81

Fig 5.30 – The velocity profiles and stress distribution under the wrong boundary conditions	81
Fig 5.31 – The velocity profile and y-velocity distribution at transient state under 4000 Pa	82
Fig 5.32 – The shear stress and pressure distribution at transient state under 4000 Pa	82

Chapter 1. Introduction

1.1 ISN Project

In an effort to design more advanced soldier uniforms and systems through the use of the developing nanotechnology, two years ago, MIT and U.S. Army launched the Institute for Soldier Nanotechnology (ISN) project. Although the ISN project is currently focused on fundamental science and engineering, its main goal is to develop state-of-the-art soldier system in the near future. To perform this mission, many fields from mechanical engineering to chemical engineering work together interdisciplinarily without any barrier. For classification, ISN research is divided into six team projects, almost 50 projects in detail. Among these projects, we are in Team 4: Biomaterials and Nanodevices for Soldier Medical Technology.

1.2 Team 4 Project

Research Projects are as follow:

Project 4.1: Switchable surfaces

Project 4.2: Non-invasive diagnostics and delivery of injury intervention agents

Project 4.3: Semi-active variable-impedance materials: biomechanical design and control

Project 4.4: Nanostructured biomedical fiber constructs

Project 4.5: Field responsive fluids for load transfer in splints and other medical devices

Among subgroup projects, we are in Team 4.3 and 4.5 in collaboration with Prof. Mckinley's research group. Our long-term goals are to design with semi-active variable-impedance materials to minimize power and weight in military applications such as body armor and splints. Such materials could make body armor more effective and could be used for first-aid splints to protect wounded soldiers on the battle field. Currently ER and MR fluids for these applications is being studied by many researchers and some applications have already been invented and tested, from automatic machine tools and automotive shock absorbers to digital camera in cellular phones. Moreover, due

to recent advances in ER fluids, we have investigated the properties of ER material to check whether this can be used for military purposes, such as protect the soldier. In addition to military application, this material could be used for any other purposes. For example, one might make ski boots or skates fit to the foot more easily by inserting ER fluid between fabrics and then activate an electric field, tightening the shoes.

The primary goals of our research are to investigate the ER fluid and to build the proper models and designs through both experiment and simulation. In this thesis, the simulation is based on the three simple modes in case of Newtonian fluid and Bingham plastic fluid by using the FEM software, ADINA. And simulations are compared with experimental results to check their validity.

1.3 Thesis overview

This thesis describes fundamental research regarding semi-active variable-impedance materials. Basically, it focuses on the simulation of electrorheological (ER) fluids in several geometries and three operating modes. To simulate the ER fluids, the properties of Bingham plastic fluid and Newtonian fluid were surveyed and used. Moreover, various boundary conditions of different conditions were tested to see if these conditions fulfill the properties of ER fluids. The contents of each chapter are briefly explained as following:

Ch2 – Introduction to the background of Electrorheological fluid: history, definition, properties, mechanisms, classification and applications, and description of Magnetorheological (MR) fluid

Ch3 – Explanation of the Finite Element Method(FEM) and introduction to the Galerkin method used by ADINA to calculate the equations, and a brief description of the ADINA software modules which were used in my FEM calculations.

Ch4 – Explanation of mathematical models of the behavior of ER fluids in three basic operating modes - shear, pressure and squeezing mode. Also a description of how to build FEM designs and how to choose the boundary conditions in each case.

Ch5 – Presentation of the FEM results, discussion and conclusion of the results in each case.

Also a description of future work

Chapter 2. Electrorheological fluid

Intelligent (smart) materials can adaptively change or respond to an external environmental stimulus, i.e. electric or magnetic field, photon irradiation or ionic strength, in a timely manner, producing a useful effect [1]. A critical parameter such as yield stress which is able to be controlled by simply changing the external environment can be used to generate a special function. Electrorheological (ER) fluid is one of the smart materials which changes its flow properties in response to an electric field [8], while magneto rheological (MR) fluids can be controlled by an external magnetic field. This chapter introduces ER and MR fluids and provides a background on proposed mechanisms for the ER effects.

2.1 Historical background and definitions

2.1.1 History of ER fluids

The Electrorheological effect, sometimes called the “Winslow effect”, was first reported in detail by Willis Winslow in 1949 [3]. It was reported that the application of an electric field to nonaqueous silica suspensions activated with a small amount of water caused rapid solidification of the originally fluid material. He envisioned the fluid being used in numerous electromechanical devices such as clutches, brakes, and valves that could be actively controlled by an electric field [30]. While this exciting effect has produced extensive research, few commercial applications have been found due to various limitations in material properties such as temperature restrictions, settling out of suspension, and lack of range of viscosity [18, 26]. These disadvantages have prevented the ER fluids from being developed as practical applications, despite its 50 years-long history.

MR fluids are considerably less well known than their electrorheological (ER) fluid analogs. Both fluids are non-colloidal suspensions of polarizable particles having a size on the order of a few microns. The initial discovery and development of MR fluids and devices can be credited to Jacob Rabinow at the US National Bureau of Standards in the late 1940s [21]. Interestingly, this work was almost concurrent with Winslow's ER fluid work. The late 1940s and early 1950s actually saw more

patents and publications relating to MR than to ER fluids [21]. However, for the last two decades, new types of ER materials such as liquid crystal polymer-based fluids or core-shell structured particle based fluids have shown stronger effects than the typical ER fluids. Moreover, recently the new kind of ER materials with giant electrorheological effects may overshadow the disadvantages of ER fluids [8].

For more than half a century, smart fluids have been little more than a laboratory curiosity. But gradual improvements in their properties—the development, for example, of additives that prevent suspended particles from clumping or settling—and recent advances in the systems used to control them have led to the first commercial applications in cars, bridges and even digital cameras [17].

2.1.2 Definition and applications

Definition

The term “smart fluid” is generally applied to fluids whose properties can be changed by the application of an electrical or magnetic field. In particular, there are electro-rheological (ER) and magneto-rheological (MR) fluids that can change, in an instant, from free-flowing liquids to become more viscous, or even solid. ER fluids consist of tiny dielectric particles dispersed in an insulating fluid such as silicon oil, while MR fluids use magnetisable particles suspended in a non-magnetisable carrier liquid. Normally, the particles are randomly aligned. But when an electric field is applied, they are aligning along it, forming long chains that make the liquid more viscous. This process is amazingly reversible: once the field is removed, the fluid flows freely again. And by varying the field, the fluid's viscosity can be carefully controlled [17].

Usually, ER fluids show dramatic changes in rheological properties, when an external electric field is applied. ER fluids are generally recognized as behaving according to the Bingham plastic model for fluid flows, meaning that they will behave as a solid up to a certain yield stress. At stresses higher than this yield stress, the fluid will flow, and the shear stress will continue to increase with the shear rate, so that,

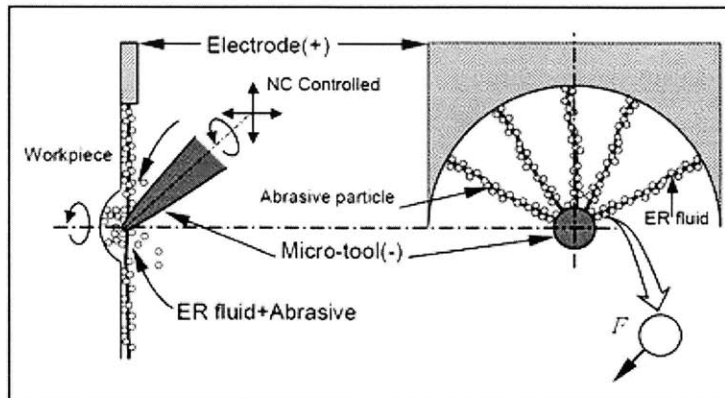
$$\tau = \tau_y + \mu\dot{\gamma}$$

, where τ_y is the shear yield stress, τ is the shear stress, $\dot{\gamma}$ is the shear strain rate and μ is the dynamic viscosity. In general, both the yield stress and the viscosity will be functions of the electric field strength.

Applications

The basic properties of electro- and magnetorheological fluids as well as various models for electro- and magnetorheological fluid devices, especially vibration dampers, and their applications have been discussed in this paper. However, there is still a need for rigorous mathematical models which accurately describe electro- and magnetorheological fluids and devices, and which are suitable for understanding, investigating and predicting their behavior by numerical simulation. Furthermore, to fully utilize the innovative potential of adaptively controllable electro- and magnetorheological fluid devices, (optimal) control strategies must be developed taking into account the dynamical behavior of the specific complex mechanical system including the controllable ER or MR fluid device. For example, when using a semiactive suspension based on controllable ER fluid shock absorbers, the full dynamical behavior of the vehicle, the ER fluid dampers and the road disturbances must be considered in order to maximize the driving comfort and the safety of a car by adaptive damping and level control. For this purpose, models for actively controllable ER and MR fluid devices must be developed describing the dynamical behavior of a specific device with respect to changes in the electric or magnetic field.

Even though ER fluids have some limitations or disadvantages over the MR fluids, steadily they have been developed for commercial uses from the automobiles to the digital cameras. In the automobile industry, ER damper has been tested for the alternatives of the shock absorber. Recently, researches have shown that cars with semi active ER dampers had better performance in terms of stability and handling than cars with current or traditional dampers [30]. Moreover, to reduce engine noise, engine mounts with ER fluids has been studied and it has been shown that the new engine mounts have better performance in terms of noise insulation [30]. The Anti-lock brake system (ABS) is also another application [31]. In the manufacturing industry, ER fluids have been investigated for more precise polishing and finishing [33,34].



<Fig 2.1- Overview of the polishing using ER fluid [29]>

This thesis describes one of the projects to use this material for body armors or first-aid splint for wounded soldiers. Moreover, better ER performance would make ER fluids suitable for sports accessories. As seen in some of the examples mentioned above, the applications using smart fluids have large potential and great versatility. Their advantage, novel and unique properties are enough to attract the attention of scientists and engineers. However, there are still some problems with the use of the materials, for example durable operation at high temperature, ER attrition due to long uses and instability from the sedimentation, etc. If these barriers are overcome, the ER fluids will be used more widely.

2.2 Classification of ER fluid

The ER fluid can be classified by two methods. One classification is based on the relationship of shear stress and shear strain rate (functional classification) and the other is on the basis of particle existence (Particle-based classification).

2.2.1 Functional classification

Positive Electrorheological Fluids

Positive ER fluids display a positive proportional relationship between stress and strain rate upon application of an electric field. Desirable characteristics of ER fluids include [1],

- (i) a high yield stress – larger than 5 kPa under an electric field of 2 kV/mm
- (ii) a low current density passing through the ER fluid – less than 20 $\mu\text{A}/\text{cm}^2$
- (iii) a strong ER effect within a wide temperature range– from 30 °C to 120 °C
- (iv) a short response time, usually less than 10^{-3} s
- (v) a high stability and no particle sedimentation or material degradation.

Negative Electrorheological Fluids

Negative ER fluids display an inverse by proportional relationship between stress and strain rate. Upon application of an electric field, the shear viscosity is lower than that of disperse phase. This phenomenon is thought to be caused by the Quincke rotation [1]. When particles immersed in a semi-insulating liquid are submitted to a sufficiently high DC field, they can rotate spontaneously around any axis perpendicular to the field [52]. As a result, rotating particles makes the flow rate reduced, so that the apparent shear viscosity is decreased. This rotation occurs in DC and AC fields, but only over the threshold of electric field strength. A criterion for evaluating the negative effect and the positive effect was proposed, which was based on the physical parameters of both the dispersed and dispersing materials [1].

Photo-Electrorheological Fluids

Some materials, called PER-active materials, can change their own viscosity positively or negatively with optical illumination. Water is supposed to play an important role in this effect: high water content exhibits a negative ER effect, while low water content shows the reverse phenomenon. Photo-generated carriers were thought to change the electric properties of changing the ER performance. Thus they can make the ER performance changed. For example, TiO_2 is one of the materials that have this effect [1].

2.2.2 Particle-based classification

Typical ER fluids are made from colloidal suspensions whose properties depend strongly and reversibly on an electric field. The difference in dielectric constants between the fluid and particles is thought to be one of the main reasons for this effect. Upon application on an electric field to the ER fluid, the randomly scattered particles are aligned along the electric field, which makes ER fluid to have yield stress, viscosity and other properties. However, newly developed materials for the last two decades need another categorization. They can be split into two categories according to water

content: hydrous or anhydrous ER materials. Water limits the operating temperature range, raises conductivity, and accelerates device erosion. However, anhydrous ER materials has another disadvantages i.e. particle sedimentation, which could make ER fluids malfunction [1]. To get rid of these disadvantages, liquid/oil or liquid miscible homogeneous ER fluids have been developed, which do not have any particulates, or which have composite core-shell structured particles which mainly have an inorganic core shelled or modified polymer, and they have been investigated for the improvement ER effect and fluid stability [1].

Heterogeneous Electrorheological fluids

This category, which is also called particle based ER fluids, includes ER materials which contain micro-sized conducting inorganic particles such as Aluminosilicates, conductive organics and polymers such as oxidized polyacrylonitrile, carbonaceous materials, Fullerenes, or superconductive materials, e.g. $\text{YBa}_2\text{Cu}_3\text{O}_{7-x}$ [1]. This also includes the core-shell composite based ER materials.

Aluminosilicates are one of the commonly used particles due to their strong ER effect. However, they have some shortcomings such as sedimentation or device abrasion by hard particles [1]. To overcome these shortcomings, organics or polymers can be developed for better dispersion, but the ER effect is weak compared to that of inorganic particles.

The particles are usually irregularly-shaped (size = 0.5-100 μm) and present at concentrations of 10-40% by mass. ER fluids are composed of conducting particles and an insulating medium (such as silicone oil), along with additives (such as surfactants, dispersants, and possibly a polar activator), which can show electropolarization upon an electric field application. The electric field can be either AC, pulsed DC, or DC, but AC could produce less electrophoresis of particles to electrodes [4].

Homogenous Electrorheological fluids

Before 1985, most ER materials contained particles, and could not overcome the problem of particle sedimentation, even though some suitable surfactants were introduced. To overcome this shortcoming, liquid materials were often used as the dispersants dissolved in the insulating oil. The former is immiscible, the latter is miscible. In the case of oil-in-oil emulsion systems (immiscible), stretched droplets that form fibrillation chains are found to show an ER effect. Chlorinated paraffin/polydimethylsiloxane is one of the examples for the dispersed liquid. Liquid crystal polymer(LCP)/oil systems, which is another type of immiscible materials, also show a strong ER effect. In the case of miscible systems, low molecular weight LCP could show the ER effect by

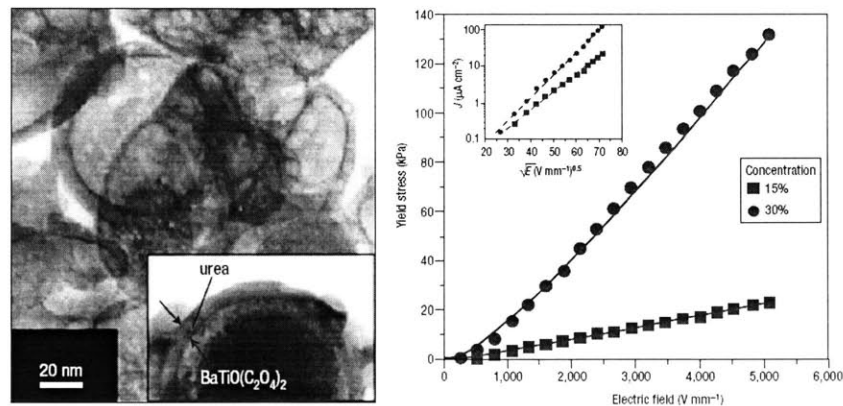
itself or upon dissolution in another liquid medium. In contrast to immiscible homogeneous ER materials, miscible homogeneous ER materials show a weak ER effect (from 1.7 to 3.0 kPa) [1].

Although a lack of sedimentation makes these homogeneous materials promising, they have other shortcomings such as high viscosity under zero electric field and liquid-liquid segregation problems occur. In addition, in the case of LCP, only the nematic phase, among possible three phases can show an ER effect [1].

In this research, typical particle based ER fluids and LCP based homogeneous ER fluids were investigated.

2.2.3 Gigantic ER fluid

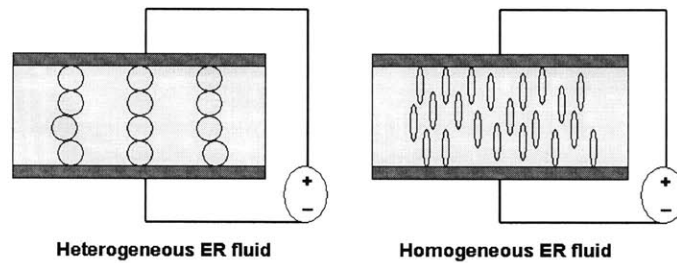
Recently, a report regarding the breakthrough of a novel ER fluid was published from Hong Kong researchers [8]. This newly developed ER fluid shows a high yield stress of 130 kPa at 5kV/m, while the limit of typical ER fluids is 20 kPa, which was thought to be the barrier [8]. This fluid is made with silicone oil as a suspension and nano-sized particles, Barium titanyl oxalate(BaTiO_3), coated with Urea[8]. The picture of this fluid which was characterized by the gigantic positive ER effect and the core-shell composite particulate was showed in figure 2.3 . However, the larger ER performance makes this discussed here separately. The particles are 50~70 nm in average and each has surface coating of 3~10nm. Notably, the static yield stress displays near-linear dependence on the electric field, in contrast to the quadratic variation usually observed [8]. These extraordinary outstanding properties of ER materials might expedite the development of ER application devices.



< Fig 2.2 Gigantic ER fluid – image of particles(left) and static yield stress vs. electric field (right) [8]. >

2.3 Mechanisms and Properties of ER fluid

The mechanisms of heterogeneous ER fluids cannot be explained by simple physical theory because ER effect results from several different reasons. The main reason is that the particles align along the electric field due to the electric dipole moment and form the fibrillated structures, while they are randomly scattered at zero electric field. However, this cannot fully describe the dominant ER effect of some other materials when organic materials, polymers, carbonaceous materials and Fullerenes are suspended. Other reasons such as water content, diffusion theory and polymer hydrodynamics are thought to play a role as well. In this thesis, several physical theories are explained briefly. In case of the homogeneous ER fluids, the nematic phase of Liquid crystal polymers (LCP) and their changes in orientation angle along the electric field have been ascribed for this performance.



< Fig 2.3 - The mechanisms of two different ER fluids >

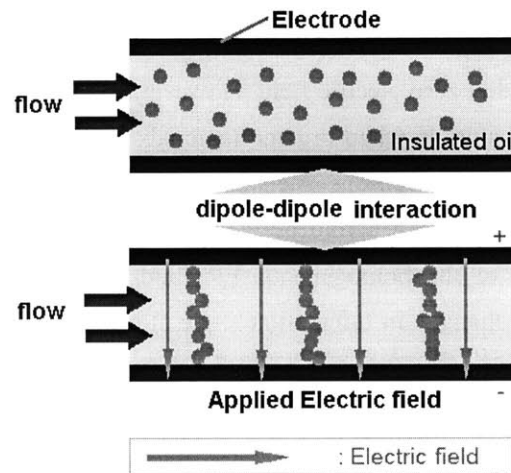
2.3.1 Heterogeneous ER fluids

Some researchers have reported that the electric dipole or the electrostatic polarization is the main reason for this ER phenomenon. However, this is not the only force acting on the particles. Other physical mechanisms have been also proposed for the origin of the ER response: interelectrode circulation, double-layer overlap and water bridging [7].

Electropolarization

The electrostatic polarization mechanism attributes the origin of the ER effect to the field-induced polarization of the disperse phase particles relative to the continuous phase. In this model,

polarization can arise from a number of charge transport mechanisms, including electronic, atomic, dipolar, nomadic, or interfacial polarization [7]. Suppose that the dielectric constant of the suspended particles is larger than that of the solvent. An electric field then polarizes the particles, leading to the appearance of induced charge at the particle surfaces. This charge creates a dipole moment, aligning the particles along the electric field and making a structure called fibrillation.



< Fig 2.4 - Electropolarization >

Other mechanisms

Other mechanisms such as interelectrode circulation, double-layer overlap and water bridging can also be one of the reasons for the ER effect. The former two models are based on the energy dissipation and the latter is based on the water bridges which influence the potential of particles. If more additional energy is needed to start to flow, in terms of Rheology, it could be said that the ability to interrupt the flow is increased so that it can show some ER effect. In case of the interelectrode circulation, suppose that the particles move rapidly back and forth between the electrodes and that the particles have the ability to change the sign of its charge rapidly. The secondary flow is generated by the external electric field and the additional energy dissipation [4, 7].

Double layer theory can explain what effect by using the deformation of the diffuse part of the double layer which is composed of the distinct monolayer and the diffuse thick layer. The distinct monolayer is closely adhered to the solid surface and this thickness is one ion thick, while the diffuse thick layer can extend some distance into the liquid. When the diffuse part is deformed by the external field the velocity gradient, the velocity gradient can dissipate the extra energy or the particle interaction, repulsion or the overlap of the double layers can dissipate the greater shear

energy [4, 7].

Water also plays an important role in the ER effect, because most ER fluids have some water even if they are nominally anhydrous. Moreover, water is the main reason why the operating temperature is limited. When the field is applied, the water resides in the gap where the electric field strength is much larger than nominal field strength, and by linking two spheres such as bridges, water could influence the cohesive force between particles. If the surface of particles was rough, water content could strongly influence particle interactions. When the field is removed, the water retreats due to surface tension or disjoining pressure [7].

Properties

To describe the hydrodynamic behavior of ER fluids, the yield stress and dimensionless number was introduced. Yield stress usually is proportional to the square of the electric field strength, which is almost consistent with the theory-expected value which is calculated from the electrostatic polarization [1,2,3,4,7].

The Mason dimensionless number has been also used to explain the ER fluids. It describes the ratio of viscous to electrical forces, and given by

$$Mn = \frac{24\pi\epsilon\mu\dot{\gamma}}{(\beta E)^2}$$

,where μ is viscosity, $\dot{\gamma}$ is shear strain rate, β is the effective polarizability and ϵ is the solvent dielectric constant [4,7]. In the case of the Bingham plastic fluid, the shear stress can be expressed by

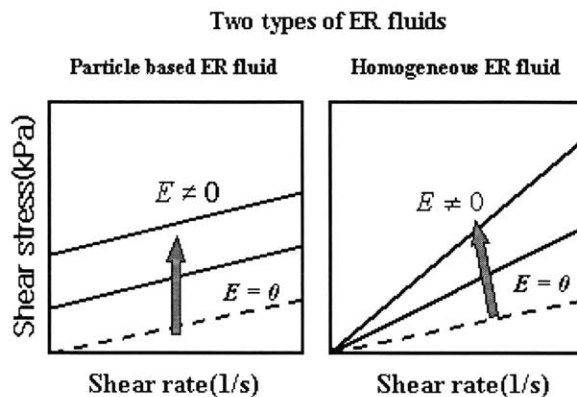
$$\tau = \tau_0 + \mu\dot{\gamma} = \tau_0(1 + aMn),$$

,where a is a numerical constant ~ 1 [4].

2.3.2 Homogeneous ER fluids

ER fluid of this type was developed with liquid crystalline polymers and exhibit characteristics as shown in Fig. 2.4. The shear stress nearly proportional to shear rate is generated, and its slope, namely viscosity, can be controlled by an electric field. As a result, it is possible to acquire a mechanical control force proportional to the speed under a constant electric field and to mechanically realize what is equivalent to the so called differential control. While the heterogeneous ER fluids can be described by the Bingham fluid, the homogeneous ER fluids can be modeled by the Newtonian fluid. Therefore the particle based ER fluids increase the yield stress

with increasing electric field. On the other hand, LCP based ER fluids change their own viscosities by the external electric field.



< Fig 2.5 Stress-shear strain rate relationship of two different types >

Comparing these two types of ER fluids, the homogeneous ER fluids are much better than the heterogeneous fluids in terms of the generated shear stress and operating temperature [15, 23, 24, 25]. Following table 2.1 shows differences between the heterogeneous and homogeneous ER fluids. Moreover, the LCP-based ER fluids outperform the particle based ER fluids in terms of shear yield stress. In some cases, the shear stress is more than ten times better [24]. However, according to the Inoue's report, various types of LCP diluted with DMS shows a large ER effect, while pure LCP never shows the effect and this phenomenon occurs for many types of LCP [15].

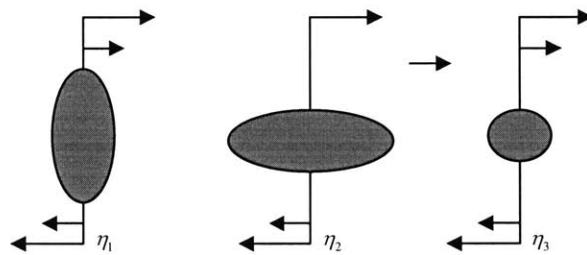
ER fluid type	Heterogeneous	Homogeneous
Rheological behavior	Bingham flow	Newtonian flow
Generated shear stress(Pa) (the shear rate is 300 sec ⁻¹ at 2kV/mm)	600	8000
Viscosity(poise) (Under no electric field)	1	10
Response(msec)	<3	20~80 (rise)
Operating Temp. (°C)	0~60	10(or 0)~60
Current density(μA/cm ²)	<1	1 ~ 2

< Table 2.1 comparison of two types of ER fluids which are made by Asahi Kasei [15] >

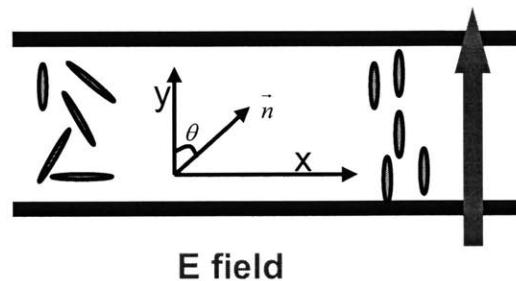
Mechanisms

The primary reason for the ER effect is the reorientation of liquid crystal polymer along the electric field. LCP consists of a rigid core and flexible tail(s) which form liquid crystal phases over certain temperature ranges. LCP can have different phases according to its structure: nematic, smectic and cholesteric. Among these phases, only the nematic phase can show the significant ER effect. The temperature required to maintain the nematic phase depends on the polymer. In the case of nematic phase, Miesowicz defined viscosities for the three principal orientations in simple shear flow experiments (figure 2.6) [26]. LCP could be modeled as a three dimensional oval so that they could have three different axes. From figure 2.6, Of these three viscosities, η_1 has stronger viscosity than the other two types. Moreover, the increased aspect ratio of LCP increases the ER effect.

When an electric field is applied, the nematic phase LCP can change its angle orientation (figure 2.7), which increases the viscosity, In other words, accompanying structural changes are rheological changes. Ericksen and Leslie provided an explanation in the form of the continuum theory for the rheology of liquid crystals [4]



<Fig 2.6 - Three different Miesowicz viscosities of LCP>



< Fig 2.7 - The reorientation of LCP by the electric field>

2.4 Magnetorheological fluid

Magnetorheological (MR) fluids are materials that respond to an applied magnetic field with a change in rheological behavior. The MR effect is the dual of the ER effect with magnetic fields rather than electric fields [17]. MR fluids are composed of magnetizable particles and an insulating fluid (see table 2.2). Typically, this change is manifested by the development of a yield stress that monotonically increases with the applied magnetic field [21].

Particle	ferromagnetic or ferromagnetic magnetically nonlinear particles including iron, nickel etc. ($1 \mu\text{m} \sim 10\mu\text{m}$)
The medium	Organic or aqueous liquids
Advantage	higher maximum shear stress, use practical electric source, unaffected by impurities
Disadvantage	less stable , irreversible , heavier than ER

<Table 2.2 MR fluids [21]>

Except for a flurry of interest after their initial discovery, there has been scant information published about MR fluids. Only recently has a resurgence of interest in MR fluids been seen. While the commercial success of ER fluids has remained elusive, MR fluids have enjoyed recent commercial success. A number of MR fluids and various MR fluid-based systems have been commercialized, including an MR fluid brake for use in the exercise industry, a controllable MR fluid damper for use in truck seat suspensions and an MR fluid shock absorber for oval track automobile racing. [21]

The magnetorheological response of MR fluids results from the polarization induced in the suspended particles by application of an external field. The interaction between the resulting induced dipoles causes the particles to form columnar structures, parallel to the applied field. These chain-like structures restrict the motion of the fluid, thereby increasing the viscous characteristics of the suspension. The mechanical energy needed to yield these chain-like structures increases as the applied field increases, resulting in a field dependent yield stress. In the absence of an applied field, MR fluids exhibit Newtonian-like behavior [3, 6, 21].

Interest in magnetorheological fluids derives from their ability to provide simple, quiet, rapid-response interfaces between electronic controls and mechanical systems. Magnetorheological fluids have the potential to radically change the way electromechanical devices are designed and operated

has long been recognized [21].

Usually the MR effect is much stronger than the typical particle-based ER effect (see table 2.3) The MR effect has some advantages over ER including broader temperature and viscosity ranges, and has found limited commercial applications in dampers and clutches at Lord Corp., for example.[22]

Property	MR	ER(Particle-based)
Maximum Yield Strength	50 ~ 100 kPa	2~5 kPa
Maximum Field Strength	~ 250kA/m (limited by saturation)	~4kV/mm (limited by breakdown)
Operable Temp. Range	-40 to + 150 °C (limited by carried fluid)	+10 ~ 90 °C (ionic, DC) -25 ~125 °C (non-ionic, AC)
Stability against impurities	Unaffected	Very Sensitive
Response time	Within milliseconds	Within milliseconds
Density	3 ~ 4 g/cm³	1 ~ 2 g/cm³
Maximum Energy Density	0.1 J/cm³	0.001J/cm³
Power Supply	2~25V, 1~2 A (2~50 W)	2~5 kV, 1~ 10mA (2~50 W)

< Table 2.3 Representative controllable fluid properties from <http://literature.lord.com/root/other/rheonetic/MRvsER.pdf> >

Chapter 3. Finite Element Method

To simulate the behavior of ER fluids, the finite element analysis and its software, ADINA was used. The finite element method is a numerical analysis technique used by engineers, scientists, and mathematicians to obtain solutions to the differential equations that describe, or approximately describe a wide variety of physical (and non-physical) problems. For this reason, the finite element method (FEM) was chosen to calculate and display the complicated fluid motion, a knowledge of which is necessary to control ER fluids. Here the finite element method will be briefly explained. In addition, internal calculation in ADINA is performed with the Galerkin method which ADINA uses to solve the flow problems.

3.1 Finite Element Method

The finite element method is a numerical analysis technique used by engineers, scientists, and mathematicians to obtain solutions or the results to the differential equations that describe, or approximately describe a wide variety of physical (and non-physical) problems such as fluid and soil mechanics, electromagnetism or dynamics. Finite element methods are useful in virtually every field of engineering analysis [19]. In FEM, a physical problem is converted to the mathematical model with some assumptions, because some simplification or idealization could make use of the mathematical equations to solve this problem [19, 27]. During numerical calculation of fluid problem in ADINA, the Galerkin method was used, which was used for solving integral equations such as the exterior electric field problems over the electric surface. In terms of numerical analysis, in order to solve Navier-stokes equations efficiently, FEM software use this method to reduce the order of differential equations. In this chapter, the finite element method and the Galerkin method were explained briefly.

3.1.1 Finite element method

The underlying premise of the method states that a complicated domain can be sub-divided into a series of smaller regions in which the differential equations are approximately solved. By

assembling the set of equations for each region, the behavior over the entire problem domain is determined. Each region is referred to as an element and the process of subdividing a domain into a finite number of elements is referred to as discretization. Elements are connected at specific points, called nodes, and the assembly process requires that the solution be continuous along common boundaries of adjacent elements [49].

The FEM procedures can basically be separated into 7 steps[49]. Most steps, especially preprocessing steps, can be performed automatically using a software package. However, to simplify the model and determine the proper boundary conditions are up to the software users. Here the brief procedure can be described.

Discretization

A fluidic motion is one of the motions in continuous domain like any other natural motions. To solve this motion in computer-aided calculation, we should discretize this domain into the simply disconnected elements. This discretization can be different from the regions. If we are more interested in central region, we could use much smaller mesh size to express precisely. Today, state-of-the-art software packages automate the meshing process [49]. In case of ADINA, the meshes were generated after the material properties and element groups were chosen. The number of nodes per elements is 9, which is usually used. For example, one rectangular element has 9 nodes, i.e. four vertices, four middle points of the edges and the center of the rectangle. Three nodes per elements could get the same result, but this could distort the deformation so that this was not used specially in case of fluid problem.

Interpolation functions & Element properties

Once an element shape has been chosen, the analyst must determine how the variation of the field variable across the element domain is to be represented or approximated. In most cases, polynomial interpolation function is used. The number of nodes assigned to an element dictates the order of the interpolation function which can be used. Interpolation functions are also referred to as shape functions or approximating functions [49].

The simplest method of approximation is to assume a linear distribution of the unknown function within the element domain. Most one-dimensional functions can be represented as a series of straight lines. The smaller the line segments, the more accurate the solution will be. Conversely, the larger the line segments, the less accurate the solution will be. Computational costs, on the other hand, may increase significantly as the number of elements in a model increases. Thus, it may be

more practical to use fewer elements, and ones that have a higher order of interpolation [49].

Once the interpolation functions have been chosen, the field variable in the domain of the elements is approximated in terms of discrete values at the nodes. Consequently, a system of equations is formed which expresses the element properties in terms of quantities at the nodes [49, 50].

Assembly of the element properties

The assembly procedure combines each element approximation of the field variable (as defined in the previous steps) to form a piecewise approximation of the behavior over the entire solution domain. Assembly is accomplished using the following basic rule of compatibility: The value of the field variable at a node must be the same for each element that shares that node. This step is handled automatically by the finite element package [49, 50].

Boundary Conditions

most equations cannot be solved without any boundary equations, as if we can get the family curve of the differential equations by using the arbitrary constant. Mathematically, before applying the boundary conditions, the system of equations is indeterminate and does not have a unique solution. If the boundary conditions are incorrect or the wrong boundary conditions are applied, the result could be different in the same geometry. In the case of ADINA, a fixed boundary condition, a loading boundary condition and a special boundary condition such as moving wall could be applied to the geometry. Moreover, instead of the normal traction condition, we could use the displacement as a kind of applying forces. In this case, a specific displacement at a specific time could be applied.

Solving the system of equations

Once the boundary conditions have been applied to the assembled matrix of equations, standard numerical techniques can be used to solve for the unknown field variable at each node. Basically, most equations could arrive at the form of $\mathbf{Ax} = \mathbf{B}$, which is standard linear form. After that, numerically, a Gaussian elimination could be used. If the structure of A is symmetric or sparse matrix, then the speed of calculation or efficiency could be faster and the storage of the data could be reduced. Many solution methods make use of these properties to provide fast and efficient computation algorithms which are now implemented in nearly all finite element packages. In ADINA, the LU decomposition is used to solve the system equations.

Post-processing

This step could be different by the purpose of FEM software users. Based upon the solution to the field variable, additional calculations include the computation of principal stress, strain energy and dynamic responses in a structural analysis. In flow analysis, the stress distribution and the velocity profile can be calculated. In ADINA, ADINA-plot shows the result of post-processing.

3.1.2 Galerkin method

To solve many problems in the fluid mechanics, the governing equations, the so-called Navier-Stokes equations, need to be solved. However, these equations are so complicated that in most cases simplifying assumptions must be made such as incompressible or steady case in order to simplify the system of equations. In ADINA, the actual calculations are performed by using the weak form of the Navier-Stokes equations or Galerkin finite method.

In case of reducing orders, the weak form of the differential equation is used. While the strong statement is the form of differential equations with boundary conditions, the weak statement or the weak form has the integrated form using the weight function and boundary conditions. For example, (D. V. Swenson, ww2.mne.ksu.edu/classes/ME862), in case of the one dimensional elastic rod, the strong form is

$$AE \frac{\partial^2 u}{\partial x^2} + b = 0 \quad \text{for } 0 \leq x \leq L \quad (3.1)$$

,where A is area, E is Young's modulus, u is the displacement ,b is the internal body force and L is the length of the rod.

with the boundary conditions:

$$u = 0 \quad \text{at } x = 0 \quad (3.2)$$

$$AE \frac{du}{dx} = F \quad \text{at } x = L \quad (3.3)$$

After integrating both terms with boundary conditions and a weight function (w), (3.1) can be converted into the weak form as following:

$$AE \int_0^L \frac{dw}{dx} \frac{du}{dx} dx = \int_0^L w b dx + w(L)F \quad (3.4)$$

In any case, the weak statement is equivalent to the strong statement [28]. The reason why the weak statement is used to solve equations in FEM software is that the order of the differential equations can be reduced by one and this procedure can make the matrix formulation symmetric, increasing computational efficiency and reducing the storage requirements. In addition, it allows for the use of piecewise functions for u , i.e. it can weaken the requirements of differentiability. Moreover, the natural boundary conditions are included in the analysis.

To solve this equation, the Galerkin or collocation method is used. Both methods can be used to solve the integral equations, however, ADINA usually uses the Galerkin method to solve this equation. Suppose the approximation solutions consist of functions such as

$$u_n = \phi_0 + \sum_{j=1}^n a_j \phi_j \quad (3.5)$$

where u_n, ϕ_j is the n -th piecewise function of u and j th approximation function. After inserting this into (3.4), the following formula can be achieved.

$$AE \int_0^L \frac{d\phi_i}{dx} \left(\frac{du}{dx} + \sum_{j=1}^n a_j \frac{d\phi_j}{dx} \right) dx = \int_0^L \phi_i b dx + \phi_i(L)F \quad i = 1, \dots, n \quad (3.6)$$

This can be transformed into the form $Ax = b$.

The Navier-Stokes equations for the incompressible viscous flow are

$$\frac{\partial \vec{u}}{\partial t} - \nu \nabla^2 \vec{u} + (\vec{u} \cdot \nabla) \vec{u} + \nabla p = \vec{f} \quad \text{in } \Omega \quad (3.7)$$

where \vec{u}, p, \vec{f} and ν are the velocity, the pressure, the external forces and kinematic viscosity respectively and Ω is the flow region. The continuity equation is

$$\nabla \cdot \vec{u} = 0 \quad \text{in } \Omega \quad (3.8)$$

To define the relationship between (3.5) and (3.6), the initial condition and boundary condition must be considered.

$$\vec{u}(x, 0) = \vec{u}_0(x) \quad \text{with } \nabla \cdot \vec{u}_0 = 0 \quad (3.9)$$

$$\vec{u} = \vec{g} \quad \text{on the surface with } \int \vec{g} \cdot \vec{n} d = 0 \quad (3.10)$$

, where \vec{n} is the outward unit vector to the surface.

After integrating and using the Galerkin method, the discretized weak form is obtained:

$$\nu \int_{\Omega_h} \nabla \vec{u}_h : \nabla \vec{w}_h dx + \int_{\Omega_h} ((\vec{u}_h \cdot \nabla) \vec{u}_h) \cdot \vec{w}_h dx + \frac{1}{2} \int_{\Omega_h} (\nabla \cdot \vec{u}_h) (\vec{u}_h \cdot \vec{w}_h) dx - \int_{\Omega_h} p_h (\nabla \cdot \vec{w}_h) dx = \int_{\Omega_h} f \cdot \vec{w}_h dx \quad (3.11)$$

$$\int_{\Omega_h} (\nabla \cdot \vec{u}_h) q_h dx = 0 \quad (3.12)$$

, where p_h, q_h are suitable approximation functions for the Galerkin method [48].

3.2 ADINA

ADINA is general purpose FEM software to solve complicated problems in electromagnetics, heat transfer and structure analysis. It has been developed by Prof. Bathe at MIT. Like other finite element software packages, it can be separated into three parts: data input module (pre-processing or preprocessor), solution module (solver), and results module. The solution module has four different modules to solve different cases (see table 3.1).

Module name	Description
ADINA-F	CFD program for the analysis of compressible and incompressible flow with state-of-the-art capabilities for moving boundaries and automatic remeshing.
ADINA-T	Module for the heat transfer analysis of solids and field problems.
ADINA-FSI	The ADINA-FSI (fluid structure interaction) program is the leading code used by industries for fully coupled analysis of fluid flow with structural interaction problems. This module is available to users who license both the ADINA and ADINA-F modules.
ADINA-TMC	This module provides capabilities for thermo-mechanical coupled (TMC) analysis, including analysis of contact with heat transfer.

<Table 3.1 - ADINA modules extracted from <http://www.adina.com/products.shtml>>

In case of Solid, ADINA module provides many standard models such as elastic, plastic, viscous materials, etc. However, the Bingham plastic model wasn't provided. A geo-technical model, which has the perfectly plastic properties, could be used but the material properties related with this model have not been known so that this model couldn't be used. With the same reason, the viscous model couldn't be used. Hence, to simulate solid region in Bingham plastic fluid, plastic model with having bilinear properties were used. In the case of fluid, ADINA-F can solve the fluid problem. In this thesis, the heat problems were not considered. ADINA – FSI can solve the fluid-structure interaction with using both ADINA and ADINA-F. When the fluid influenced on the structure, this module was used, but when the structure had influence on the fluid, ADINA-F was not enough to simulate it in the squeezing mode.

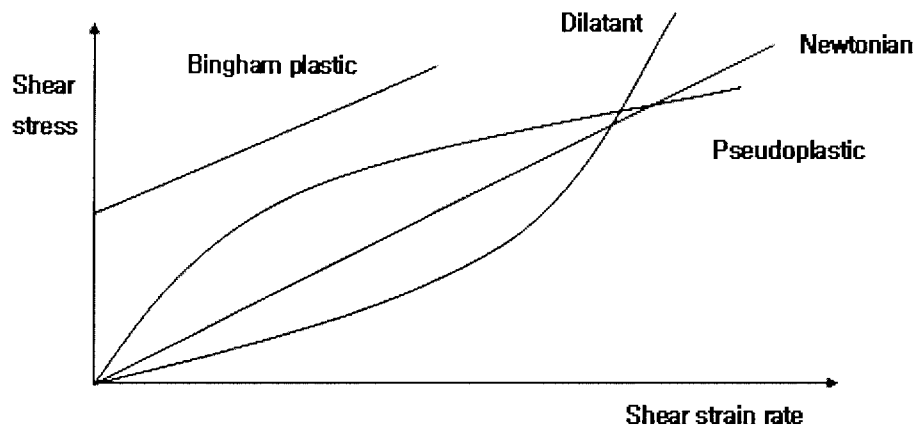
Chapter 4. Mathematical modeling and FEM simulation

When an electric field is applied to ER fluid, the fluid can have properties of solids and fluids. Under yield stress, it can behave like a solid, which means that its behavior can be characterized by Young's modulus. On the other hand, over the yield stress, ER fluids flow like highly viscous fluids, so that it can be explained by flow motions. The Bingham plastic fluid could be one of the simple models which can describe this material with properties of a solid and a fluid. This chapter will describe Bingham plastic fluid and its FEM modeling.

4.1 Mathematical modeling of the ER fluid

4.1.1 Bingham plastic fluid and Newtonian fluid

When we categorized all fluids in terms of rheological properties, all fluids are divided into two categories: Newtonian and non-Newtonian. Newtonian fluids are those liquids which show a linear relationship with zero offset between shear stress and shear rate. Mineral oil, water and molasses are examples from this category [51].



<Fig 4.1- The relationship of Newtonian and non Newtonian fluids between shear stress and shear rate >

On the other hand, a non-Newtonian fluid has a different relationship between shear stress and strain rate. Pseudoplastic liquids, which are very common, display a curve starting at the origin again and curving up and along but falling under the straight line of the Newtonian liquid. In other words, the increasing shear rate results in a gradual decreasing shear stress or a thinning viscosity with increasing shear. Toothpaste and whipped cream are good examples. Unlike pseudoplastic liquids, dilatant liquids give a curve which curves under then upward and higher than the straight line Newtonian curve (Like a square law curve). Such liquids display increasing viscosity with increasing shear. A wet sand and mixtures of starch powder with small amounts of water belong to this categorization [51].

A Bingham plastic fluid can be defined as a material that behaves as a rigid body at low stresses but flows as a viscous fluid at high stress. Heterogeneous ER fluids or particle-based ER fluids (which are most common) consist of conducting silica particles and non-conducting oil. In the microscopic region, ER fluids are micro-structured liquids whose rheological properties undergo a rapid change in less than a millisecond in response to an external electric field. When an electric field is applied, the polarization of conducting particles results in the ER effect. Therefore, simulations of ER fluids are based on the molecular dynamics while also including other mechanisms contributing to the ER effect [12]. However, in the macroscopic region, heterogeneous ER fluids show the similar behavior to Bingham plastic fluids and can be modeled with the properties of Bingham plastic fluids. Based on Bingham plastic fluids, the relationship between shear stress and shear strain rate can be obtained. Among these relationships, Bingham plastic fluid and Newtonian fluid can be represented by the following simple power-law formula [51].

$$\tau = \tau_y + \eta_p (\dot{\gamma})^n \quad (4.1)$$

Shear stress = Yield stress + plastic viscosity * (shear strain rate)ⁿ

Where $\tau_y = 0$, $n=1$: Newtonian Fluid

$n \neq 1$: Non-Newtonian Fluid

$n > 1$: Dilatant fluid

$n < 1$: Pseudoplastic fluid

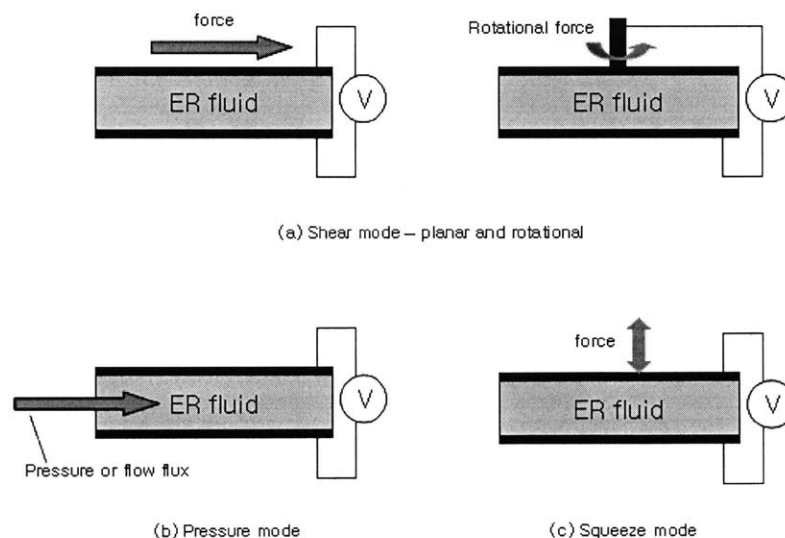
$\tau_y \neq 0$, $n=1$: Bingham Fluid ex) Slurry, Wax

n≠1: Non-Bingham Fluid

On the other hand, LCP-based homogeneous ER fluids or homogeneous ER fluids cannot be modeled by a Bingham plastic fluid even though they show a similar ER effect. Their ER effects result from the change of their own viscosities. As a result, it is possible to acquire a mechanical control force proportional to the speed under a constant electric field and to realize mechanically what is equivalent to the so-called differential control [10]. Shear stress is nearly proportional to shear rate and its slope, a viscosity, can be controlled by an electric field. Therefore, it can be simply modeled by a Newtonian fluid, while the heterogeneous ER fluids can be described by using Bingham plastic fluid.

4.1.2 Three basic motions of ER fluid applications

ER fluids are applicable with one of three basic modes or a combination of three basic modes: Shear mode or rotational shear mode, flow or pressure mode and squeeze mode. The shear modes can be applicable when one plate is fixed and the other plate is moved or rotated such as a clutch or certain smart sandwich beams, etc. The second mode can describe the ER fluidic motion when the ER fluid flows between fixed plates or into a pipe, such as a valve, an engine mount or a shock absorber is applicable to this motion. The last mode describes the flow motion which is vertical to the motion of electric field. This mode is useful to explain the flow motion when the flow between electric panels is very small.



<Fig 4.2 – Three basic flow modes>

To do macroscopic mathematical modeling of several modes, the following governing equations are needed:

Continuity equation (Mass conservation)

$$\frac{D\rho}{Dt} + \rho \nabla \cdot \vec{V} = 0 \quad (4.2)$$

Navier-Stokes Equation (Momentum conservation)

$$\frac{D\vec{V}}{Dt} = -\frac{1}{\rho} \nabla p + \vec{g} + \frac{\mu}{\rho} \nabla^2 \vec{V} \quad (4.3)$$

In addition, some following assumptions are required to be considered: incompressible, quasi-steady state (because Reynolds number is very small), No gravitational force. These ER fluids are supposed to be used in the normal environment so that we can simplify N-S equations with using these assumptions.

First, ER fluids are able to be supposed to be incompressible. Typically, oil or water is the main part of ER fluids so that it can be considered as incompressible in the typical environment because oil and water are incompressible. At second, they are considered as the quasi-steady, which means that their flows could be independent of time so that their behaviors are almost similar to the steady-state case. Hence all terms related with time could be removed. To determine this, the Reynolds number is used.

$$\text{Re} = \frac{\rho UL}{\mu} \quad (4.4)$$

Considering the experimental setting values for the shear test which is performed with collaborations,

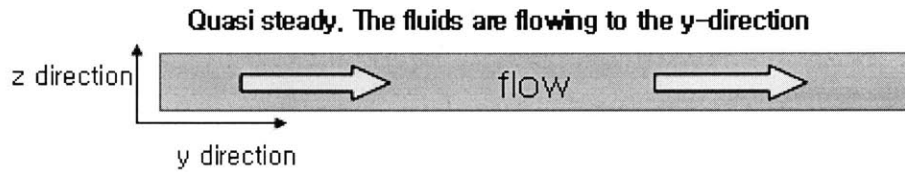
$$\begin{aligned} \text{Re} = \frac{\rho UL}{\mu} &\approx 2 & \rho &= 1100 \text{ kg / m}^3 \\ & & \mu &= 0.15 \text{ Pa}\cdot\text{s} \\ & & U &= 2 \text{ m / s} \\ & & L &= 100 \mu\text{m} \end{aligned} \quad (4.5)$$

,where ρ is the density, μ is the viscosity, U is the upper plate velocity and L is the characteristic length (height). Even though we take the values of properties much larger than the real values, the result value, 2 is so small that we can ignore the time terms, i.e. we can consider it as a quasi-steady state. Finally, the gap between two plates is micro-sized so that we can ignore the effect of gravity. The actual experiments were performed at the speed of 2mm/s so that this assumption could still be valid and this assumption is also applicable to the homogeneous ER fluid.

If we use these assumptions, from the N-S equations, we can remove some terms (see figure 4.3 for the coordinates),

$$\begin{aligned} \frac{\partial v}{\partial t} + v \frac{\partial v}{\partial y} + w \frac{\partial v}{\partial z} &= -\frac{1}{\rho} \frac{\partial p}{\partial y} + \cancel{g_y} + \frac{\mu}{\rho} \left(\frac{\partial^2 v}{\partial y^2} + \frac{\partial^2 v}{\partial z^2} \right) \\ \frac{\partial w}{\partial t} + v \frac{\partial w}{\partial y} + w \frac{\partial w}{\partial z} &= -\frac{1}{\rho} \frac{\partial p}{\partial z} + \cancel{g_z} + \frac{\mu}{\rho} \left(\frac{\partial^2 w}{\partial y^2} + \frac{\partial^2 w}{\partial z^2} \right) \end{aligned}$$

(4.6)



<Fig 4.3 – the flow in y-z direction >

Therefore, the above equations can be reduced to the followings:

$$\begin{aligned} 0 &= -\frac{\partial p}{\partial y} + \mu \frac{\partial^2 v}{\partial y^2} \\ 0 &= -\frac{\partial p}{\partial z} \end{aligned} \tag{4.7}$$

Simple Shear mode

This is the most fundamental and simplest mode among ER fluidic motions. This mathematical model can be derived from the elementary fluid mechanics. In case of simple shear mode, the force is applied only at the lateral boundaries so that, there is no pressure drop along the flow. After the proper boundary conditions are considered, (4.7) can be simplified more and the result is as

following:

$$0 = \mu \frac{\partial^2 u}{\partial y^2} \quad (4.8)$$

with boundary conditions, $u(0) = 0$ and $u(L) = U$, and then the velocity profile is

$$u(y) = \frac{U}{L} y \quad (4.9)$$

If this fluid is a Newtonian fluid i.e. in case of the homogeneous ER fluid, the shear stress is

$$\tau = \mu \frac{U}{L} = \text{const} \quad (4.10)$$

In case of the Bingham plastic fluid, the shear stress will be

$$\tau = \mu \frac{U}{L} + \tau_o \quad (4.11)$$

where τ_o is the yield stress. From (4.9) and (4.10) or (4.11), the velocity profile between the plates should be linear and the shear stress should be constant.

If we have also pressure gradient in the shear mode, then the pressure term has to be considered and the results are following:

$$U(y) = \frac{1}{2\mu} \left(\frac{dp}{dx}\right) y^2 - \left(\frac{1}{2\mu} \left(\frac{dp}{dx}\right) h - \frac{U}{h}\right) y \quad (4.12)$$

$$\tau(y) = \mu \frac{U}{L} + \frac{1}{2} \frac{dp}{dx} \quad (4.13)$$

In case of Bingham fluid, after the whole region was changed to fluid, the yield stress term will be added by τ_o . Therefore, the result is

$$\tau(y) = \mu \frac{U}{L} + \frac{1}{2} \frac{dp}{dx} + \tau_o \quad (4.14)$$

Pressure mode

As the simple shear mode can be easily calculated, the analysis of the pressure mode can be carried by a straightforward extension of elementary fluid mechanics. Supposing the flow is quasi-

steady state so that their behavior can be changed so fast, then the all fluid behavior between two plates can be changed regardless of the local region where the flow exists. From (4.7) with the following boundary conditions, $u(0) = 0$ and $\frac{du}{dy} \Big|_{y=\frac{L}{2}} = 0$, the velocity profile and shear stress will be

$$U(y) = \frac{1}{2\mu} \left(\frac{dp}{dx} \right) (y^2 - Ly) \quad (4.15)$$

$$\tau(y) = \frac{dp}{dx} \left(y - \frac{L}{2} \right) \quad (4.16)$$

In case of the Bingham fluid, the yield stress term will be added by τ_o so that the result is

$$\tau(y) = \frac{dp}{dx} \left(y - \frac{L}{2} \right) + \tau_o \quad (4.17)$$

In this case, if the shear stress greater than the yield stress, i.e. $\tau(y) - \tau_o \geq 0$, then this fluid starts to flow. At this time, the critical pressure [5, 35] to cause flow will be

$$\left| \frac{dp}{dx} \right| = \frac{2\tau_y}{L} \quad (4.18)$$

If the pressure exceeds this critical level, flow will occur, and this flow will be characterized by shear of a layer near each wall while the central portion of the fluid is unyielded [5, 35].

Squeeze mode

When the gap between two plates is small and the force is applied to the plate vertically, this is called a squeeze mode. In case of Newtonian Fluid, it can be solved by using the control volume like the piston motion. However, in case of the Bingham fluid, unlike the shear and pressure modes, the squeeze mode cannot be explained well [37]. Its validity, however, is questioned if the model is applied to other modes of loading than the one used in the test. In particular, Nilsson and Ohlsson reported that values of Bingham parameters derived from shear-flow mode tests are not suitable for the calculation of the prediction of the squeeze-flow mode behavior [37]. On the other hand, the

values of Bingham parameters derived from squeeze-flow mode tests predict rather well the behavior in other squeeze-flow mode tests, except for the fact that the amplitude and the frequency dependence are not well predicted. [37]. Gartling and Pahn-thien argued that the squeeze flow cannot contain a yield surface as all previous surface assumed because in unyielded region material must move as a rigid body due to the zero rate of deformation [38]. Therefore, in other articles, the biviscous model or Herschel-Buckley model was used [39. 40]. Biviscous model assumes that fluid could have two different viscosities, i.e. high viscosity in the pre-yield region and low viscosity over yield stress. For the squeeze mode, it can show much larger ER effect (at least one order of magnitude larger) than that of the pressure or shear force mode, because the gap is decreasing and the electric field is increasing [44].

In case of Newtonian fluid, supposing two circular plates of radius R and gap size h , the continuity equation and N-S equations can be obtained as following:

$$\begin{aligned}
\frac{1}{r} \frac{\partial(ru)}{\partial r} + \frac{\partial w}{\partial z} &= 0 \\
-\frac{\partial p}{\partial r} + \mu \left(\frac{\partial^2 u}{\partial r^2} + \frac{1}{r} \frac{\partial p}{\partial r} + \frac{1}{r^2} u + \frac{\partial^2 u}{\partial z^2} \right) &= 0 \\
-\frac{\partial p}{\partial z} + \mu \left(\frac{\partial^2 w}{\partial r^2} + \frac{1}{r} \frac{\partial w}{\partial r} + \frac{1}{r^2} w + \frac{\partial^2 w}{\partial z^2} \right) &= 0
\end{aligned} \tag{4.19}$$

where w is the axial velocity, u is the radial velocity and p is pressure.

Considering boundary conditions: $u(z = \pm \frac{h}{2}) = 0$, $w(z = \pm \frac{h}{2}) = v_0$, $p(r = R) = 0$, these coupled equations get a solution:

$$\begin{aligned}
u &= u_0 \frac{4r}{h^2 R} \left(\frac{h^2}{4} - z^2 \right) \\
w &= -v_0 \left(\frac{3z}{h} - \frac{4z^3}{h^3} \right) \\
p &= \frac{6\mu v_0}{h^3} (R^2 - r^2)
\end{aligned} \tag{4.20}$$

so that the total force can be obtained from the integration of pressure term

$$F_z = \frac{\pi R^4 v_0}{h^2} \left(\frac{\rho v_0}{4} \right) \quad (4.21)$$

It shows that the force increases with increasing radius and decreasing gap. If we consider the electric field and the axial displacement by δ , the total force should be

$$F = F_p + F_e = kf \frac{\pi R^2}{h} \left(3\mu \frac{R^2}{a^2} v_0 + E\delta \right) \quad (4.22)$$

where a is the radius of particle, E is the electric field strength, f is the volume fraction of particles and k is the absorbed volume in columns, which has a value between 0 and 1 [44].

4.1.3 Other fluid modeling

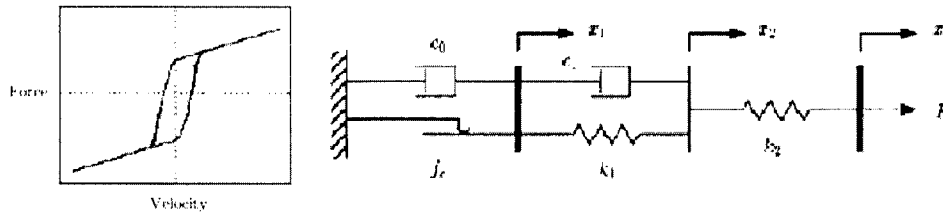
Most commonly the behavior of ER fluids is described by the Bingham plastic model as it was already mentioned above. An ideal Bingham body behaves as a solid until a minimum yield stress is exceeded and then exhibits a linear relation between the stress and the rate of shear or deformation [41]. Bingham plastic model have two parameters : yield stress and viscosity of the fluid. If these two properties are known, the basic operating mode of the ER fluid can be explained and predicted. However, it assumes that the fluid remains rigid in the preyield region. Thus, the Bingham model does not describe the fluid's elastic properties at small deformations and low shear rates which is necessary for dynamic applications [41]. Therefore here some other models are briefly introduced.

Extended Bingham model

Gamota and Filisko [42] presented an extension of the Bingham model to describe the ER fluid behavior in the pre-yield and the post-yield region as well as at the yield point. This viscoelastic-plastic model consists of the Bingham model in series with the three-parameter element of a linear solid (Zener element). The force in this system is given by three parameters

The extended Bingham model can describe the hysteric properties as shown in Fig.4.3 [43]. However, the resulting system of ordinary differential equations is extremely stiff due to the

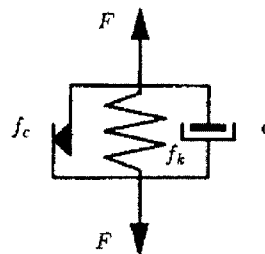
nonlinear Coulomb friction element. Thus, the numerical simulation with explicit integration methods requires very small time steps [41].



<Fig 4.4 - The extended Bingham model and the force-velocity characteristic for the extended Bingham model from [41]>

Three elements model

In that case, three elements, Coulomb friction, damper and spring were connected with parallel. The three element model predicts the experimental ER response well, and it is numerically easier to deal with than the extended Bingham model. However, it cannot always reproduce the experimentally observed variations of the forces and it shows strongly varying parameter values depending on the applied field strength and the specific external excitation [41].



<Fig 4.5 – Three element model from [41]>

Others

Bouc-Wen model, Modified Bouc-Wen model, Nonlinear viscoelastic-plastic model, Augmented nonlinear viscoelastic-plastic models could be also used for the explanation of ER fluidic behavior [41]. Bouc-Wen model was introduced to characterize the hysteric component of MR fluid damper. The hysteric component term was added to the damping and stiffness term. Modified Bouc-Wen model was introduced to allow for the fluid's dynamics of reaching rheological equilibrium. It has one more stiffness and damping terms. Damping term was connected with Bouc-wen model serially

and stiffness term was parallelly connected with Bouc-wen model. Nonlinear viscoelastic-plastic model combines a damping term with parallel-connected stiffness and another damping term In order to describe the response of an ER fluid device [41]. Augmented nonlinear viscoelastic-plastic model has two different parts: pre-yield part and post-yield part, and they were connected parallelly with the weighting function. However, due to many parameters, it is not easy to decide which one mainly influences on ER effect. What is worse, even though a parametric model is complicated, it cannot fully describe the behavior of the ER fluids. For this reason, the Bingham plastic or Extended Bingham plastic model is broadly used for the modeling [41].

4.2 Parameters of Bingham plastic

As it is mentioned above, in order to predict ER behavior, two parameters, viscosity and the yield stress are needed. The viscosity of ER fluid is one of the unique properties of each fluid which should be tested and checked by experiments, and the yield stress should also be measured. However, the estimated value of the yield stress can be predicted by theory with using the electrostatic polarization. This theory considers electrostatic force only so that the exact yield stress could be larger than the estimated value. However, the approximated value can be useful to understand the external electric field's influence. Another approach to the yield stress can be preformed by using Molecular Dynamics. It can predict viscosity and the yield stress, but in this thesis, the electrostatic polarization was considered only.

The increased strength of ER fluids is considered to reside in the attractive forces between the particles. It is now generally accepted that in most cases this forces is electrical in nature and arises from the polarization of the particles in electric field [45, 46]. In order to develop an expression of the yield stress, a system of chains of length l was considered and also a system of cross sectional A was assumed to have N_c chains and the extension by the external force is assumed to be uniform along each chain. If an external force was applied to the top of chains so that they was extended by Δl (see figure 4.6). The interparticle force (electrostatic force) along a chain, set an angle θ to the field, $F_{\mu\mu}$ was $F_{ex} = F_{\mu\mu} \sin\theta$ and the volume fraction ρ_v was defined as

$N_c / A = 6\rho_v / \pi a^2$. So the stress is

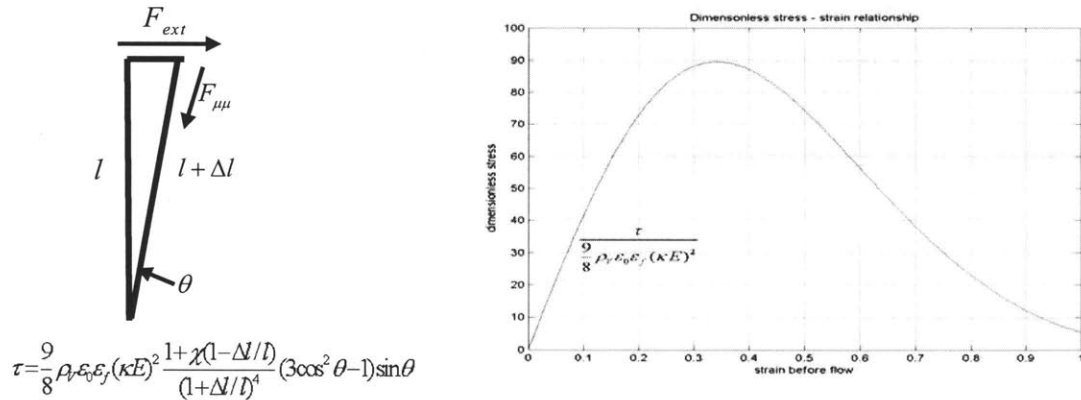
$$\tau = \frac{N_c F_{ex}}{A} \quad (4.23)$$

After inserting the interparticle force along the chain, the stress is given as following.

$$\tau = \frac{9}{8} \rho_v \varepsilon_0 \varepsilon_f (\kappa E)^2 \frac{1 + \chi(1 - \Delta l / l)}{(1 + \Delta l / l)^4} (3 \cos^2 \theta - 1) \sin \theta \quad (4.24)$$

, where ε_0 is the permittivity of particle, ε_f is the permittivity of fluid, κ is the volume polarizability, χ is the enhancement of interparticle force and E is the strength of an electric field.

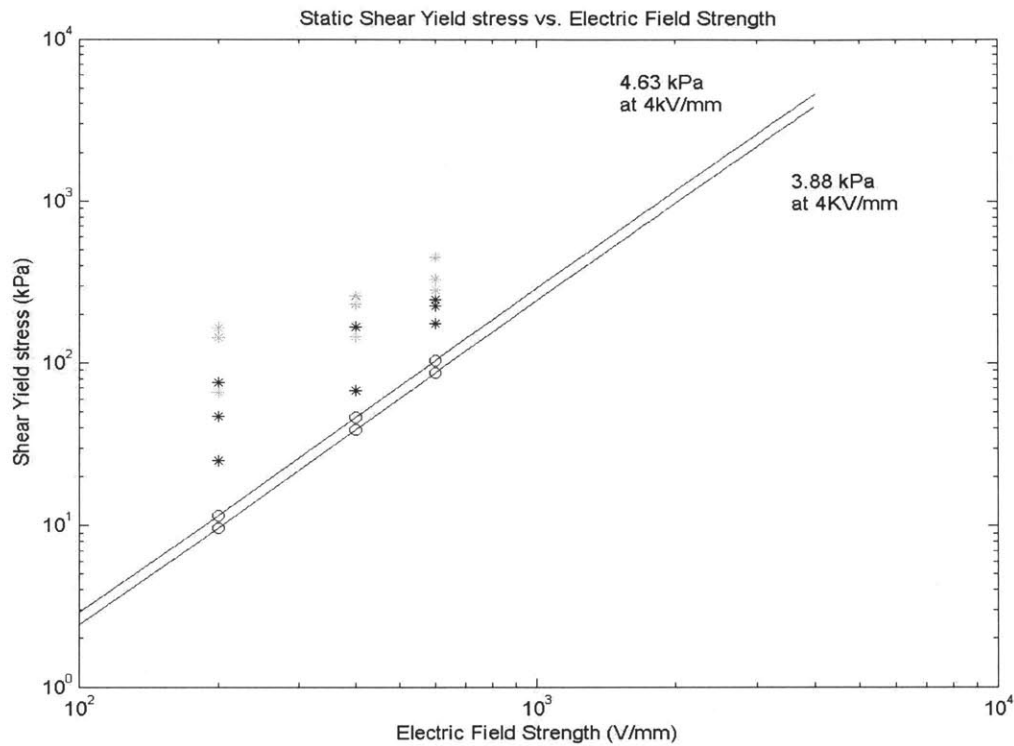
The dimensionless stress and strain part are plotted in figure 4.6 and it has maximum value at 0.35. At this point, and the particles is becoming separated by a distance. (See the formula in Fig. 4.6) At maximum point, the external force has overcome the tension (interparticle force) in the chains, i.e. the fluid start to flow. So this point could be the yield stress



<Fig 4.6 - Dimensionless stress result from the electrostatic polarization>

After this result was repeated at 0.2, 0.4, 0.6 and 4 kV/mm respectively in both cases, $\chi = 60$ and 71.6 which values could be obtained from [46], the relationship between the shear yield stress and the electric field strength was plotted in figure 4.7. The experimental data was obtained from [53], in which they were measured when the upper plate starts to move. In experiments, the small normal force was applied to measure the influence of different normal forces (4.2N and 6.2N). The experimental values (* mark) at 0.2, 0.4 and 0.6(kV/mm) are a bit larger than what we expect by theory, because we consider the electrostatic force only from the electric polarization, which is

consistent with the other journal's arguments [46]. Therefore, though the electrostatic force is the main force to ER effect, the other forces should be considered to expect more precise yield stress.



<Fig 4.7 – The theoretical prediction of the yield stress of our ER fluid:
o - the calculated data from theory [46], * - the experimental data under different normal forces from [53]. Light or green asterisks were measured at 4.2N and dark or blue asterisks were measured at 6.2N >

4.3 FEM simulations

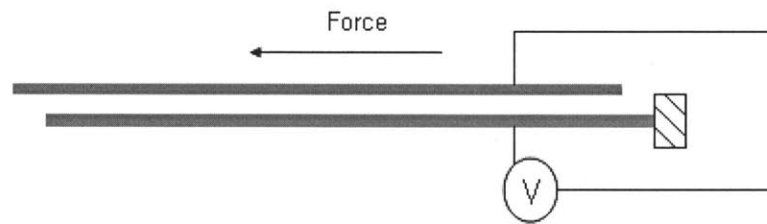
In order to investigate ER fluid behavior in several geometries, the finite element simulation is necessary, because the experiments cannot be performed in the complicated geometries. By using the FEM software, some complicated equations can be solved in many cases and from this results, another values or behavior will be predicted. To simulate ER behavior, ADINA, general-purpose FEM software, was used in this thesis. Most simulation cases have focused on the shear mode of

ER fluids because the experiment was tested on the shear mode without constant thickness. Even though ADINA can solve many complicated equations automatically, some problems cannot be solved for the deformable mesh case, which is needed to solve some squeeze mode.

4.3.1 The overview of experimental settings

Dimension of experiments

The experiments were tested with collaborations, which were focused on the shear mode in the several different spacers: no spacer, Kraft paper, tissue paper and Polypropylene. However, in this simulation, no spacer was considered. The size of electrode panel is 100 mm long and 40mm wide. (The upper plate 37mm wide to minimize the breakdown along the edges) and the gap between two plates are different from the each spacer materials, because the spacer's thickness is a gap size. In case of Kraft paper, the thickness was $4\mu\text{m}$. The Polypropylene was $8\mu\text{m}$ thick and the tissue paper is porous and $25\mu\text{m}$ thick. In case of no spacer, the thickness was variable but the average thickness was chosen around $10\mu\text{m}$.



<Fig 4.8 - Overview of the experimental setting >

Properties

To simulate ER materials, the properties of ER materials which were provided by ER fluid provider were used. Yield stress except one case was not provided so that the experimental values were used in case of the heterogeneous ER fluid. The following table shows some properties of two type fluids which were used in the experiments.

Property	Heterogeneous ER	Homogeneous ER
Provider	Bridgestone(HP-2)	Asahi Chemical Inc.
Components	Carbon-polysilicone Oil	Liquid crystalline polysiloxane

		diluted in dimethylsilicone
Rheological behavior	Bingham flow	Newtonian flow
Density(kg / m^3)	1100	800
Viscosity($Pa \cdot sec$)	0.15	10*
Response time(ms)	<2	20~80
Temperature range($^{\circ}C$)	-50~150	0~60
Characteristic stress**	Yield stress 4.2kPa at 4kV/mm	Shear stress 8kPa at 2kV/mm with shear rate , 300 (1/sec)
* is the value of viscosity under no electric field		
** Each value is provided by each provider.		

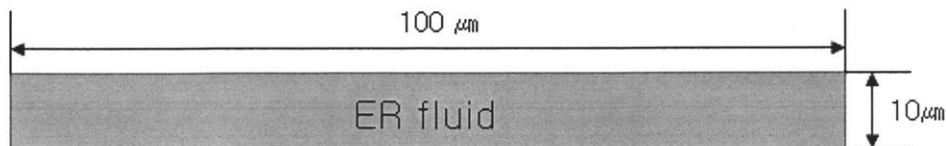
<Table 4.1 the characteristic of two types of ER fluids which are provided by both company:
Bridgestone(heterogeneous ER fluid) and Asahi Kasei(homogeneous ER fluid)>

4.3.2 FEM modeling

For my simulation, the proper geometry and boundary conditions were needed. As the illustration was showed above, the rectangles were selected as a basic geometry and the proper boundaries were chosen carefully for each simulation.

Geometry

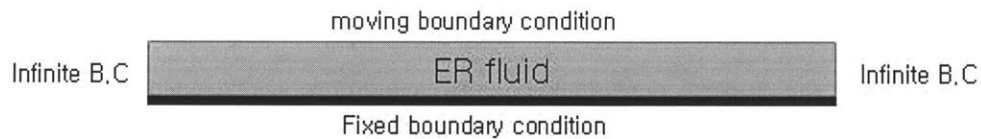
Basically, the size of rectangles is $100\mu m \times 10\mu m$ because the thickness of most tested spacer materials are less than $10\mu m$ so that $10\mu m$ was considered as the average height without any spacer. It was assumed that it would be a part of infinite plates so that the both side should have symmetric boundary conditions. In experiments, the upper plate is 100 mm long and the height is less than $10\mu m$. Its whole structure is so thin that it could be enough to simulate a part of this structure.



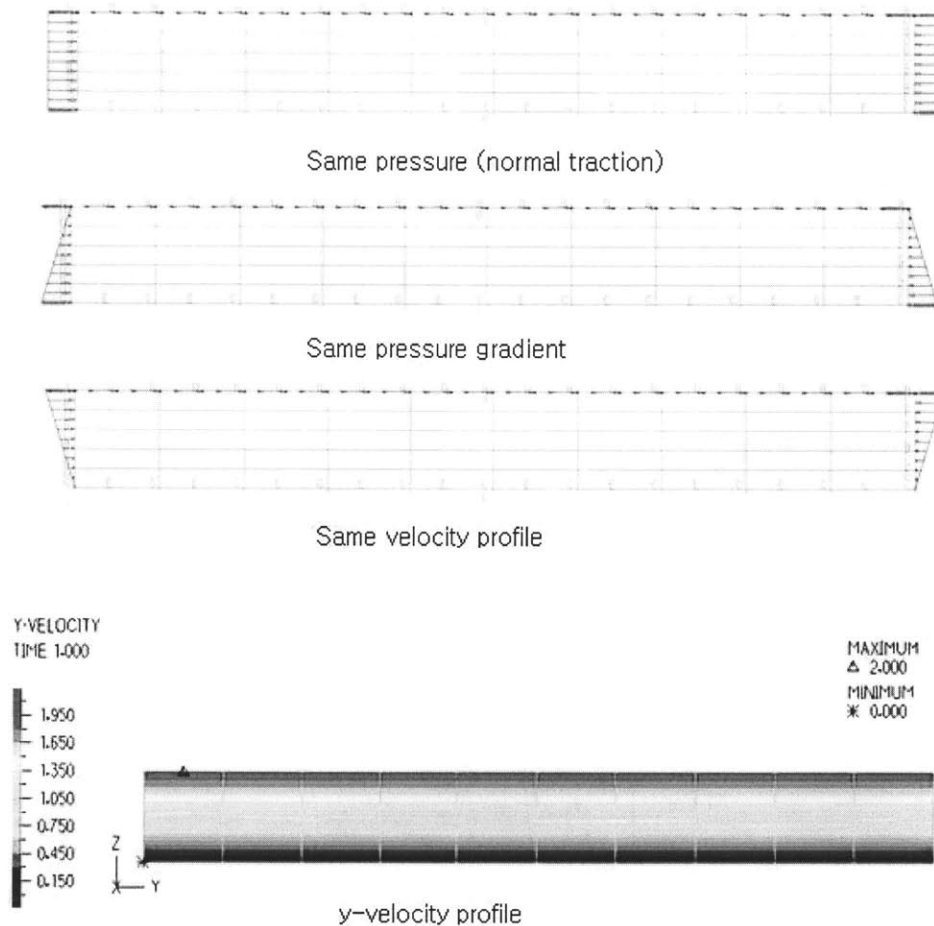
<Fig 4.9 - Dimension of the geometric modeling>

Boundary conditions

Regarding boundary conditions, all solutions of ordinary or partial differential equations depend on their own boundary conditions so that they should be chosen carefully. For example, if the external velocity applied to the upper plate with 0.002m/s, which case called shear mode is the most common case in this thesis, the upper plate has only lateral degree of freedom and the lower plate are fixed and both sides have same conditions because this FEM modeling is assumed a part of infinite structure so that both sides should have same results. To apply this condition, they might have same normal traction (pressure) or pressure gradient, same velocity profiles or any symmetric conditions. Each case showed the same result regardless of the different boundary condition (See Fig 4.11). Among these conditions, the same normal tractions are chosen because this structure is thin and the normal force to the upper plate is small so that the pressure gradient is negligible and same velocity profile could not be known except simple conditions such as simple shear flow.



<Fig 4.10 - Illustration of FEM boundary conditions>



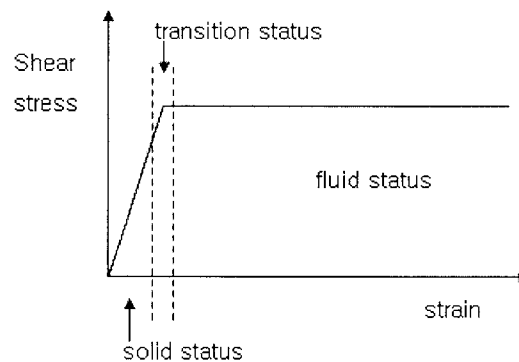
<Fig 4.11 - Three different side boundary conditions:
if the both side is symmetric, the result is always same.>

Simulation of the Bingham plastic fluid

FEM modeling discussed above is Newtonian fluid which can be applied to the homogeneous ER fluids. However, most ER fluids are heterogeneous ER fluid which can be modeled mathematically by Bingham plastic fluid. Bingham plastic fluid has both properties of solid and fluid. It looks like a rigid body under the yield stress but, it starts to flow like fluid over the yield stress. Unfortunately, ADINA software distinguishes the solid problem from the fluid problem and ADINA-F doesn't have any internal model for this like other fluid such as Newtonian fluid. In addition to that, ADINA (solid solver module) doesn't have any model for this, either. Even though

it has a similar model such as viscoelastic model or geotechnical model (perfectly – plastic model), it couldn't show any similar results as what it should be expected or the unknown properties of ER fluids were needed.

In case of the viscoelastic model, we have no information regarding the constants for Williams-Landell-Ferry(WLF) equation, which is used to relate the viscosity with temperature. Even this modulus is applicable, in case of our material whose viscosity is $0.15 Pa \cdot s$, ADINA couldn't calculate it, i.e. it has some limitations to solve this model. Another very similar model is the geotechnical material based on Mohr-Columb model which is characterized by elastic-perfectly plastic curve. However, this model just showed the elastic-perfect plastic without any shear rate and also need another unknown properties. In case of plastic bilinear modeling, we need Young's modulus and Shear hardening modulus. Young's modulus could be founded in a article [47], but shear hardening modulus couldn't. In case of our ER material there is no shear hardening modulus because it was changed into the fluid over the yield stress. However, to expect similar behavior, this model would be useful, because it can show the behavior of the plastic over yield stress and also this can show where shear stress starts to be over yield stress.



<Fig 4.12 - Three different regions of the Bingham material>

As above figure 4.11, for the modeling of Bingham plastic fluid, three divided regions could be considered. Under yield stress, it seems to be solid which can be solved by ADINA solid module. To do this, it needs shear modulus or Young's modulus and this value could be obtained from one article [47]. This is not exact same material that we used, but we might use this as rough values. For the simplification, in this thesis it was assumed that the ER material is isotropic and elastic in the solid state.

Electric field strength(kV/mm)	1	2	3
Shear yield stress(kPa)	0.3509	0.7214	0.8893
Shear modulus(kPa)	7.5463	16.0744	18.4305
Young's modulus(kPa)	20.80	46.34	55.92
Poisson ratio	0.378	0.448	0.517

<Table 4.2 Property parameters of ERM under different electric field intensities [47]>

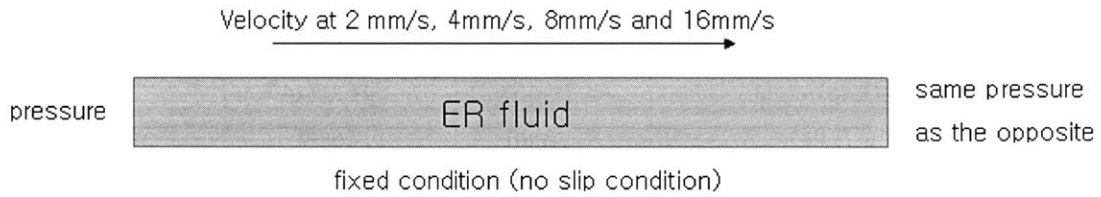
Over the yield stress, the properties of this fluid such as viscosity and shear yield stress can be used. While two regions can be solved by ADINA, the transition region is the mixed state with fluid and solid so that it cannot be explained or simulated. However, because it should satisfy the continuity, we can imagine how fluid starts to develop from solid. In case of shear mode, shear stress is same in the entire region theoretically so that the entire ER material changed its property in millisecond from solid to fluid. Therefore the transition state doesn't have to be existed. In case of the pressure mode and squeeze mode both of which have pressure gradient, the shear stress is not uniform so that the transition status should be considered until the whole entire region will be over the shear yield stress.

4.3.3 Modeling of each simulation

Basically each case was performed for Newtonian case (Homogeneous ER fluid) and Bingham plastic case (Heterogeneous ER fluid). For the pre-input data of ADINA, the properties of our tested fluid are used. If properties which we need were not be provided or known, alternatively, some properties from articles were used. All following geometric and boundary conditions were tested and some results were compared with the mathematical results or the experimental data to check whether their results are correct or not.

Simple or direct shear mode

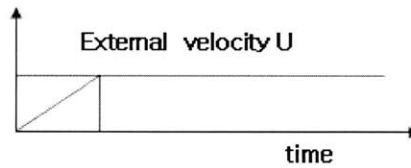
Simple shear mode is the main parts of the experiments. In this simulation, the height of the upper plate is constant throughout the regions, while the upper plates are not fixed in the experiments. However, Four different steady velocities (2, 4, 8 and 16 mm/s) were tested at the different electric fields (0, 1, 2, 3, 4 (kV/mm) with 10 μm thickness respectively)



<Fig 4.13 – The boundary conditions of simple shear mode>

Simple shear mode with increasing velocity

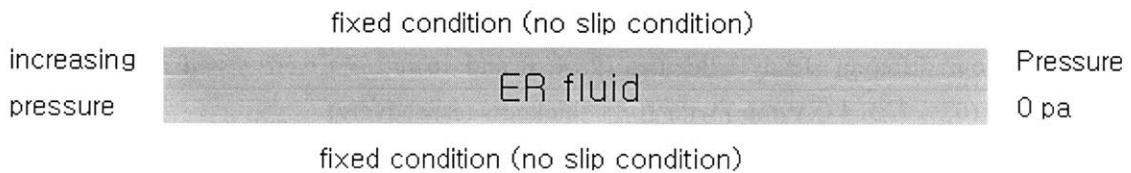
Four different velocities at 2, 4, 8 and 16 mm/s with acceleration, $10\ mm/s^2$ were tested at the different electric fields (same conditions as the simulation above). After it arrived at the target velocity, it was kept steady. To satisfy this condition in the simulation, time step was applied, i.e. to arrive at 2 mm/s , it needs 0.2 s so that the velocity profile is linear up to 0.2s and after that, the velocity was kept steady. In case of the other velocities, 0.4, 0.8 and 1.6 sec were used.



<Fig 4.14 – External velocity profile >

Pressure mode between two plates

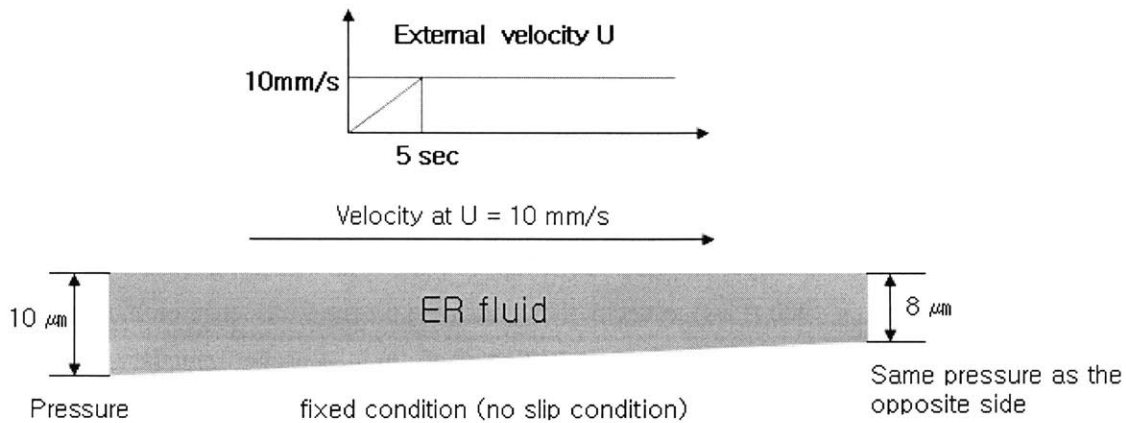
When two plates are fixed with constant pressure gradient ($\frac{dp}{dx} = -10(Pa / \mu m)$), the shear stress was tested in case of the Newtonian fluid. For the Bingham plastic case, the transition state should be considered because the shear stress is not uniform. In addition, to know where the transition state starts, the pressure was increased by 1000Pa/s at the left side.



<Fig 4.15 – Boundary conditions in the pressure mode>

Shear mode with the inclined plate (only for the homogeneous ER fluid)

When the lower plate was inclined and the velocity was increased up to 10mm/s in 5 sec and was steady after that, the shear stress was tested. Even though there is no pressure applied, the inclined panel made shear stress existed due to non-uniform pressure gradient. In addition, the thickness change of the plate may influence to the viscosity because the viscosity of the homogeneous ER fluids varies with the electric field strength. In order to test this, the changing viscosity should be also considered.

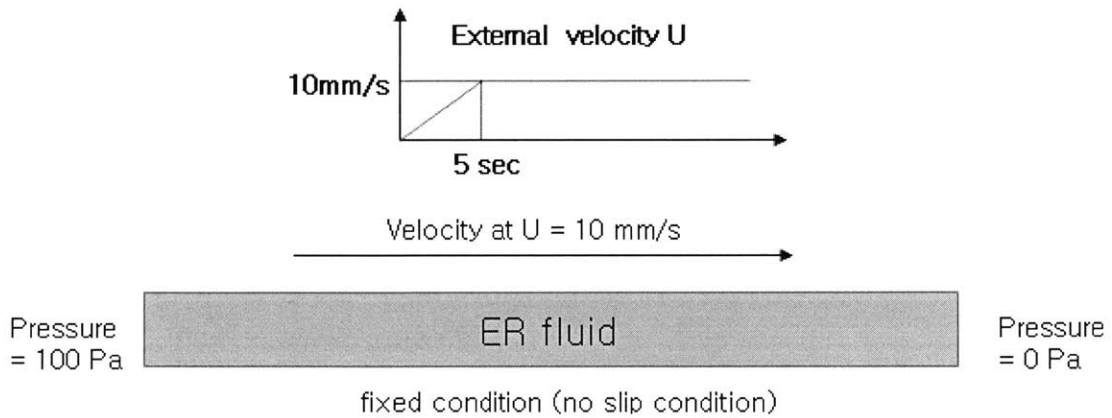


<Fig 4.16 – The external velocity profile and the boundary conditions on the inclined plate>

Shear mode with the pressure gradient

When the pressure gradient was applied to the fluid between two plates, the shear stress was tested.

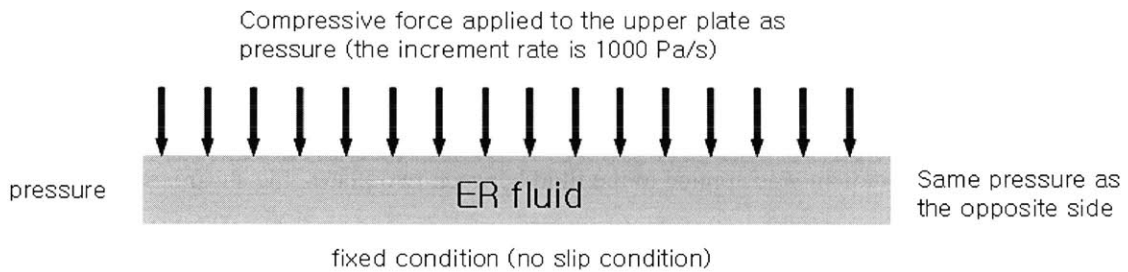
$\frac{dp}{dx} = -10(Pa/\mu m)$ means that the normal traction difference between two sides is 1000 Pa in the simulation. To test how much the pressure had influence on the velocity, several pressure gradients were checked. Also, in case of the Bingham plastic fluid, the transition case should be checked because the shear stress doesn't have same value in the entire region. The external velocity profile is following:



<Fig 4.17 – The external velocity profile and the boundary conditions with pressure gradient>

Squeeze mode test between two plates

When the compressive force was applied to the upper plate, the shear stress was tested. the pressure was increased by 1000 (Pa/s) to decide how much the pressure influence on the transition from solid to fluid in case of the heterogeneous case. Also to find the proper boundary condition, several boundary conditions were tested.



<Fig 4.18 – The boundary conditions in the squeeze mode>

Squeeze mode with the normal force

When the weights of 50, 100, 200 grams are applied on the upper plate in the normal direction and the plate was moved laterally with the velocity, 8mm/s, the effect of the normal force was checked. The total contact area is 1050 mm^2 so that the normal pressure was 47.6, 95.2 and 190.4 Pa, respectively.

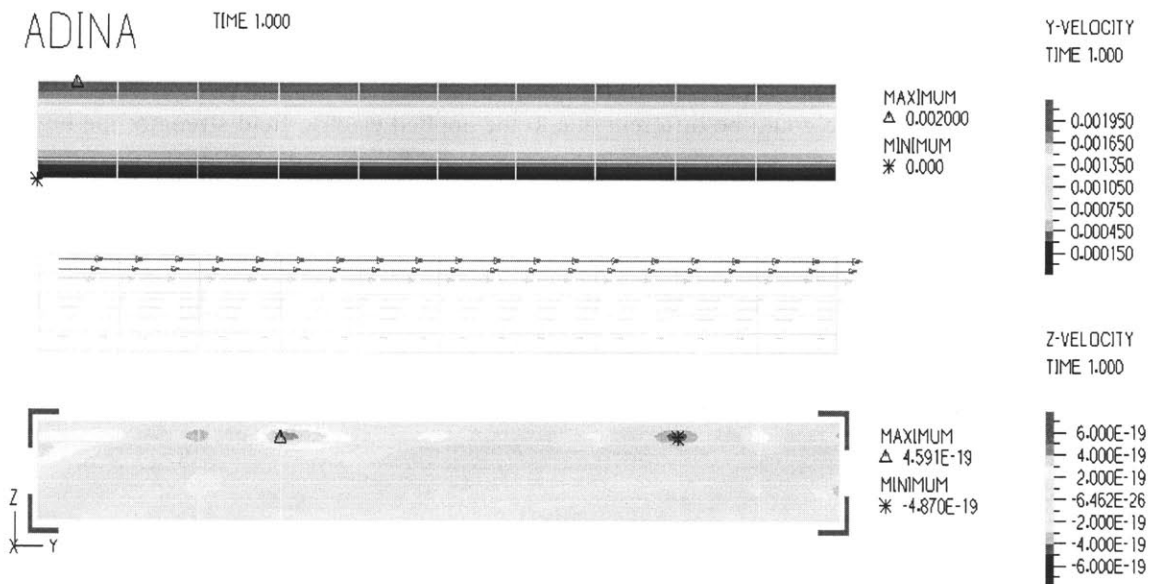
Chapter 5. Results and conclusion

From the above simulation design, some output data were obtained. After post-processing, some results were displayed visually and compared with simple mathematical modeling to check the validity of simulations. After that, the results from the Ch. 4 are summarized and several issues are discussed, and future work was proposed

5.1 Results and discussion

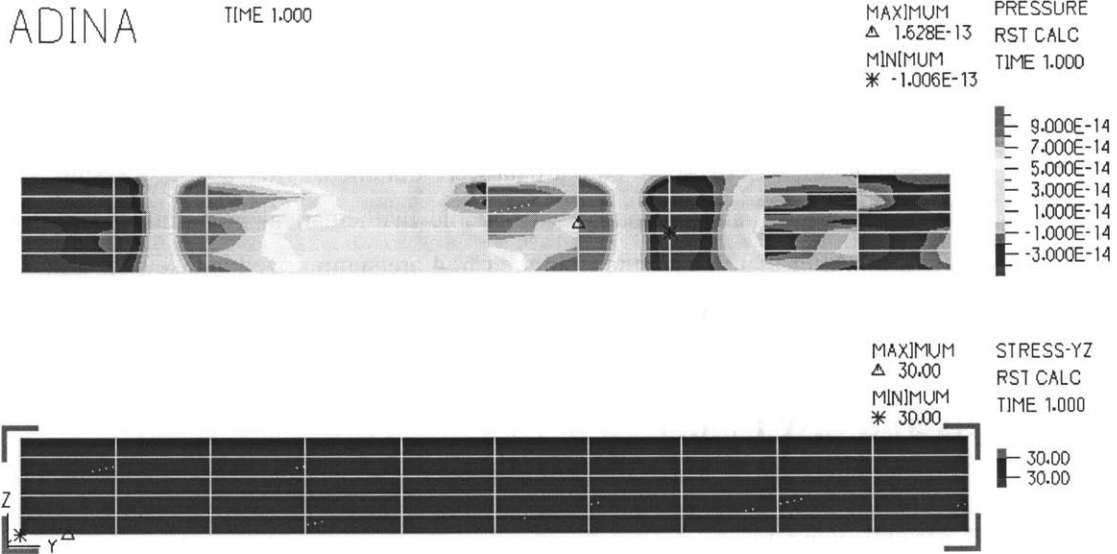
Simple or direct shear mode

Steady velocities (2, 4, 8 and 16 mm/s) were tested at different electric fields (1, 2, 3, 4 kV/mm). Simulation showed (Fig 5.1 and Fig. 5.2) that in the steady state the y-velocity is linear and the shear stress is constant throughout the region. The pressure differences are tiny and the values are over the tolerance of ADINA program so that they are negligible.



<Fig 5.1 – y-velocity profile at 2mm/s: y-velocity profile is linear and z-velocity is over the

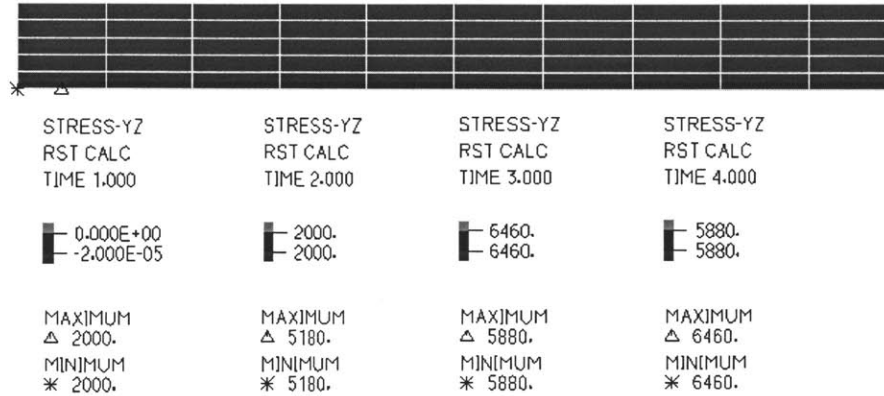
tolerance of ADINA so that z-velocity is negligible>



<Fig 5.2 – The pressure and shear stress at 2mm/s: the pressure difference is negligible and shear stress is uniform throughout the region>

In all cases, all velocity profiles are linear except they had different maximum values and the shear stress is always uniform and the values are 3, 6, 12, 24 (Pa) respectively. In the case of heterogeneous ER material, it has same viscosity under several different electric field strengths. In the case of homogeneous ER fluid, we should consider the varying viscosity. Though the velocity is same, the shear stress value could be different due to the applied electric field strength: the higher the electric field, the larger the shear stress. If the viscosity of homogeneous ER material is 10, 25.9, 29.4 and 32.3 Pa·s at 0, 1, 2 and 3 kV respectively, the shear stress at each electric field is 2, 5.2, 5.9, 6.5 (kPa). (See Figure 5.3). At the same velocity, when the applied electric field strength was increased by 1 kV/mm per second from 0 to 3kV/mm, the shear stress is also increased. (See Figure 5.3), and shear stress distribution is uniform and constant throughout the region at specific time.

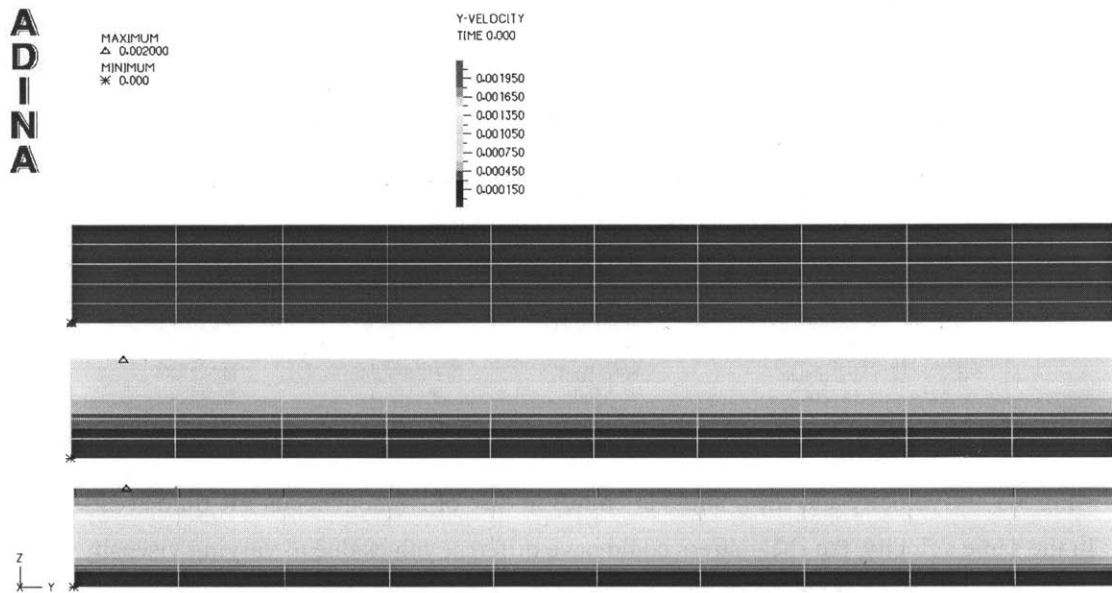
ADINA



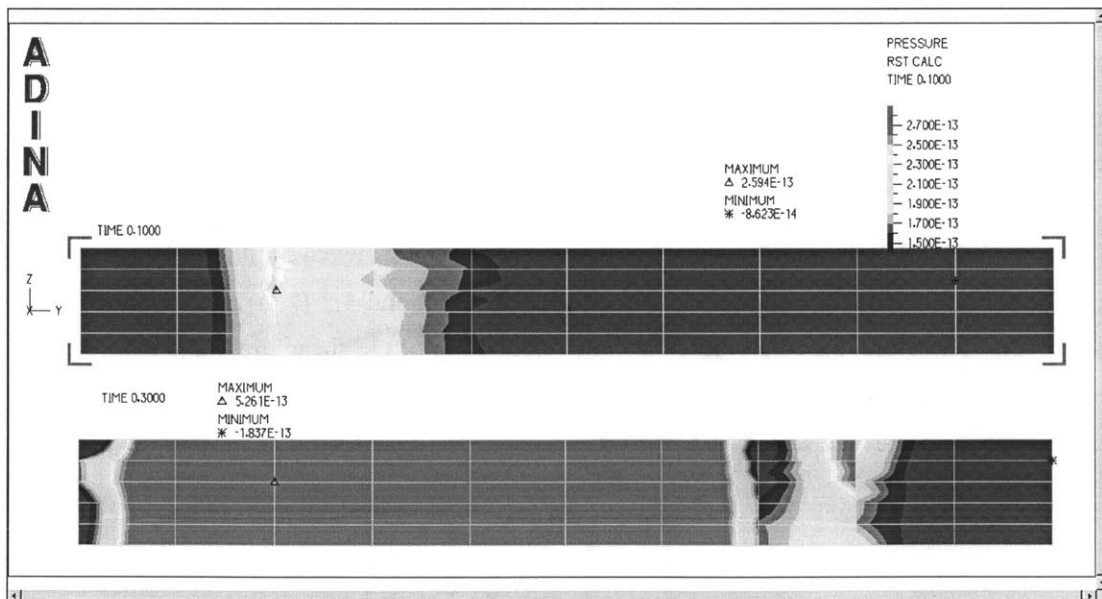
<Fig 5.3 – y-velocity and shear stress at 2mm/s in case of Homogeneous ER fluid at 2kV/mm : In the same velocity, the shear stress could have different values due to varying viscosity due to external field strength. However, the shear stress distribution is uniform>

Simple shear mode with increasing velocity

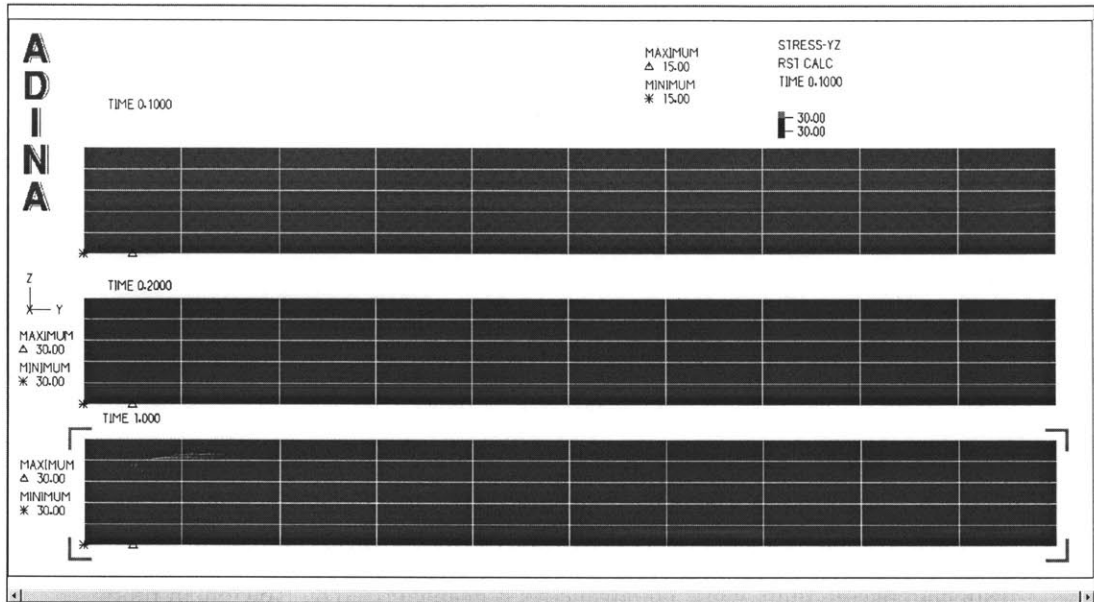
Even though the velocities were changed, the linear velocity profiles cannot be changed because their state is quasi-steady state as we mentioned in chapter 4. However, y-velocity can be checked whether it grew linearly or not (See Fig 5.4). After that, the velocity profiles are kept constant throughout the region. In the case of heterogeneous ER fluid, the shear yield stress at four different electric field strengths should be considered because it has different value in each electric field strength. From the electrostatic polarization theory, the yield stress is proportional to the square of an electric field strength, and from the fact that the shear yield stress is 0 Pa at 0V and 4.2 kPa at 4kV, the shear yield stress is supposed to be 0, 0.3, 1.1, 2.4 and 4.2 (kPa) at 0, 1, 2, 3 and 4 kV respectively. Therefore, based on these data, the relationship of the shear stress and shear rate could be plotted later (see Figure 5.7).



<Fig 5.4– y-velocity profile at 0s, 0.1s, 0.2s with the increasing velocity up to 2mm/s: the velocity propagated linearly to the lower plate. After the velocity arrives at 2mm/s, the velocity profiles are always same. >

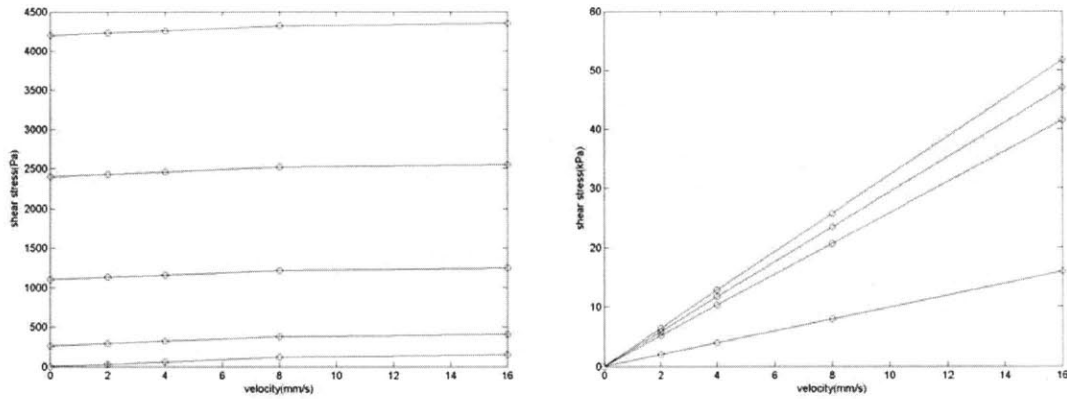


<Fig 5.5– Pressure distribution with the increasing velocity up to 2mm/s : Considering the tolerance of ADINA, it can be ignored >



<Fig 5.6– Shear stress distribution with the increasing velocity up to 2mm/s: shear stress is always uniformly constant throughout the region. the value of shear stress is only changed >

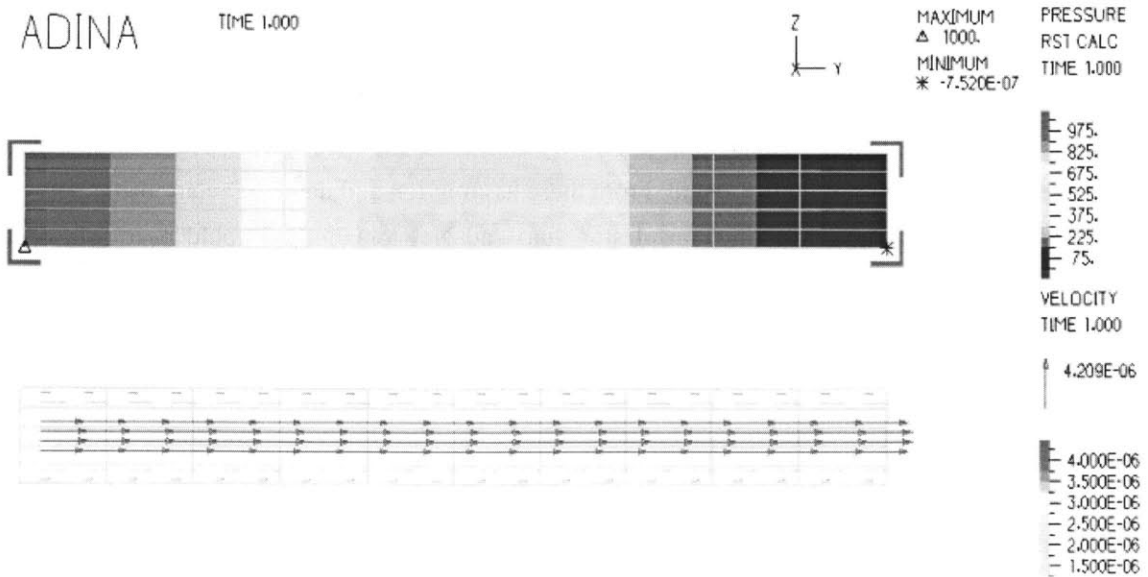
In the case of solid under the external shear force, the shear stress would be uniform and constant throughout the region. Hence, the shear stress throughout the region arrives at the yield stress point at the same time and after that, it could start to flow. Supposing that the total shear stress is the sum of the yield stress of solid and the shear stress of fluid, the Bingham plastic fluid should exhibit this behavior. On the other hand, in the case of homogeneous ER fluid, the relationship between the shear stress and shear strain rate should be linear and the slope should be changed by the external electric field strength. The value of the viscosity of homogenous ER fluid was taken from [15], in which the same material was tested. The shear yield stresses of heterogeneous ER fluid were calculated by electrostatic polarization theory which states that the shear yield stress is proportional to the square of the electric field strength. From these assumption and data, the relationship between y-velocity and shear stress of Bingham plastic fluid and Newtonian fluid could be displayed as figure 5.7. In the case of Bingham plastic fluid, it has varying viscosity by different electric field strengths. The homogenous ER fluid tested in this simulation has properties that the viscosity is changed by the electric field strength, and the changing rate of the viscosity is decreased with increasing electric field strength.

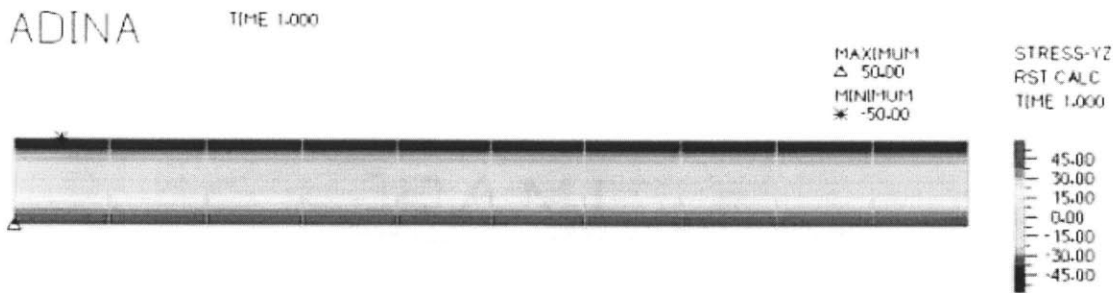


<Fig 5.7– Velocity vs. shear stress of heterogeneous ER fluid (0, 1, 2, 3, 4 kV/mm) and homogeneous ER fluid (0, 1, 2, 3 kV/mm): heterogeneous is characterized by Bingham plastic fluid, while homogeneous is characterized by Newtonian fluid>

Pressure mode between two plates

The Shear stress distribution and the velocity profile were tested when the external pressure at the left side was applied to ER fluid between two plates. In this case, a pressure gradient exists so that the velocity profile is not linear but parabolic and symmetric. In Newtonian fluids, the pressure at the center is zero and the pressure at the lowest and highest points are max. Its velocity profile, shear stress and pressure gradient at 2kV/mm are as shown in figure Fig 5.8



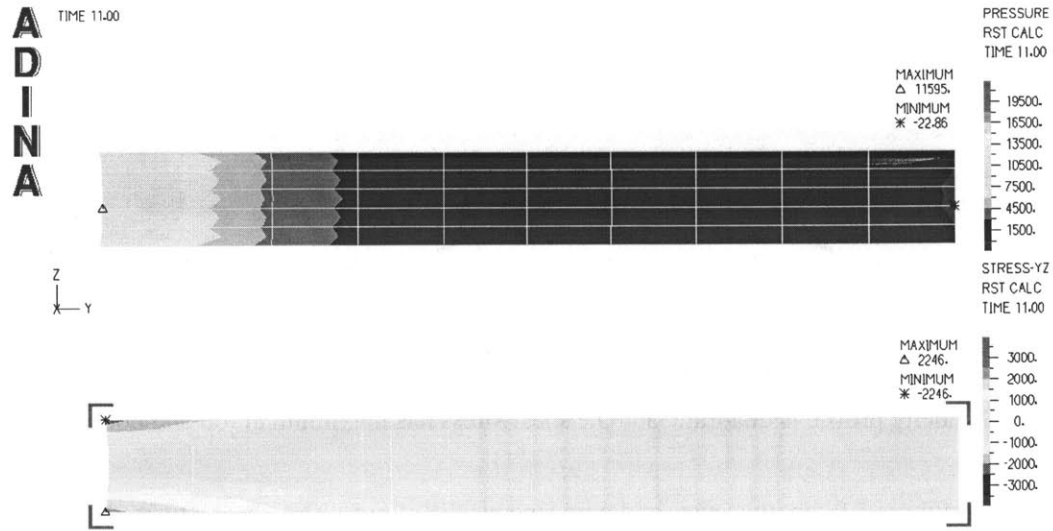


<Fig 5.8 – The pressure gradient, y-velocity profile and shear stress:

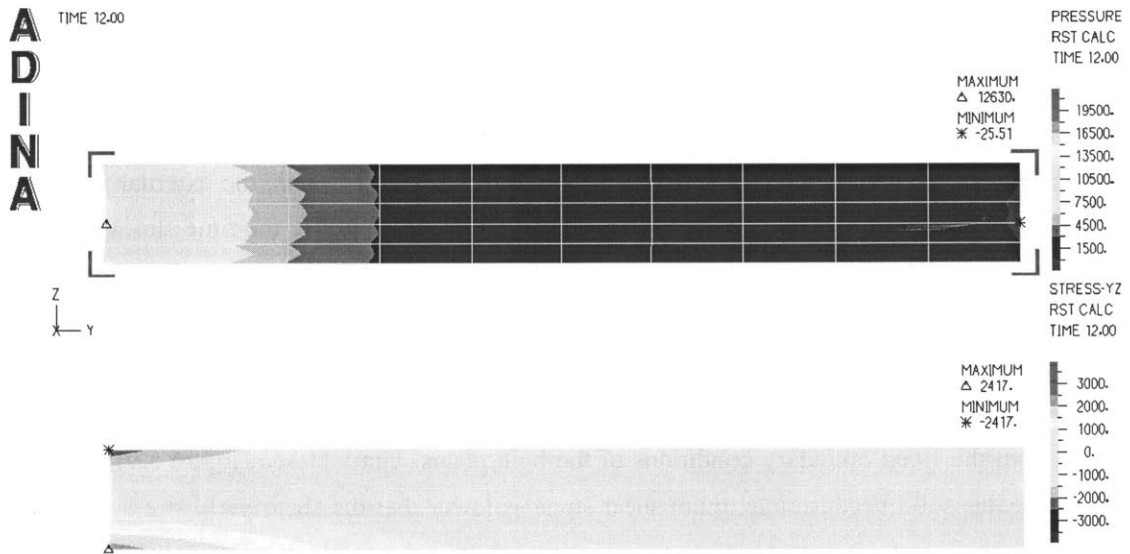
In the case of homogeneous ER fluid at 2kV/mm – the pressure is decreasing linearly, the velocity profile is quadratic and the shear stress has maximum at top and bottom. >

From the figure 5.9, in the case of homogeneous ER fluids, the shear stress distribution at arbitrary cross section is linear. It means that the shear stress at the top and bottom will be maximized so that the reorientation angle of LCP was maximized at top and bottom. At the central line, the shear stress is zero so that LCP couldn't be influenced by the external pressure and the orientation of LCP could be stayed vertical to the plate.

In the case of heterogeneous plastic fluid, in order to simulate solid and transition region, Bilinear plastic model was used. This model could be explained how the shear stress is developed and where the shear stress arrives at the yield stress at first. In order to simulate this, the external pressure at left side was increased by 1000 Pa /s. In this simulation, in order to use the time slot, the interval time, 1 sec was selected so that time has no meanings. However, by using the time slot it could indicate where the shear stress becomes larger than the shear yield stress. From the figure 5.9 and 5.10, the effect of the external pressure was propagated because the young's modulus is so small that the pressure couldn't affect the whole region in milliseconds. The displacement in the pictures results from the fixed boundary conditions of the both plates. Until 11 sec (figure 5.9), the whole region remains solid because maximum shear stress is lower that the shear yield stress (2.4 kPa at 3kV/mm). At almost 12 sec, when the pressure was 12000 Pa, the maximum value of the shear stress arrived at the shear yield stress so that the regions near those points changed into the fluid, while the other regions remain solid. After 12 sec, the shear stress was developed along the upper and low lines. From this, the first region to change their status from solid to fluid is located near the both plates at left side. Even though the transition state cannot be displayed due to the limitations, the starting point to fluid was able to be estimated.



<Fig 5.9 – The pressure and shear stress of the solid region of Bingham plastic fluid the plastic at 0.1sec, 3kV/mm>



<Fig 5.10 – The pressure and shear stress of the solid region of Bingham plastic fluid the plastic at 0.2sec, 3kV/mm>

After fully changed to the fluid, the properties of ER behavior are same as the Newtonian fluid. The velocity profile is parabolic and the velocity is max at the center. The shear stress, like the solid, at the upper and lower line, had the maximum values.

Shear mode with the inclined plate (only for the homogeneous ER fluid)

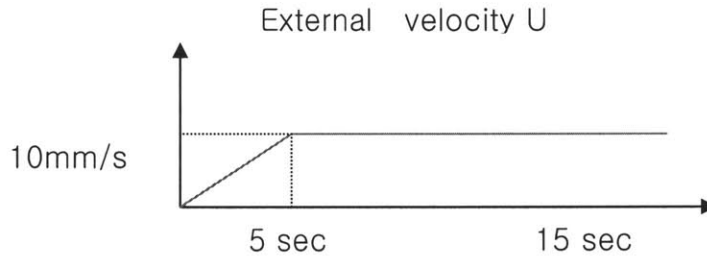
The electric field lines are not a straight line any more because lower plates are inclined so that they should have concaved line. However, because the slope of the inclined plate is not large, we can assume that the electric field lines are almost straight. Even though this assumption was allowed, in the case of homogeneous ER fluid, the viscosity change due to the electric field strength should be considered.

After the mathematical calculation from the N-S equations, the velocity profiles and pressure gradient are

$$U(y) = \frac{U}{h} y - \frac{h(x)^2}{2\mu} \left(\frac{dp}{dx} \right) \left[\frac{y}{h(x)} \left(1 - \frac{y}{h(x)} \right) \right] \tag{5.1}$$

$$\frac{dp}{dx} = \frac{6\mu U}{h(x)^2} \left(1 - \frac{H}{h(x)} \right) \tag{5.2}$$

where U is the external velocity, h is the height, p is pressure, H is the average height,



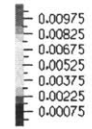
<Fig 5.11 – The external velocity profile for the shear mode with inclined plate :
until 5 sec, the velocity is increased by 2mm/s and then is kept constant >

After considering the external velocity condition (See figure 5.11) and the electric field strength (1kV/mm), the pressure gradient and y-velocity profile are as following figure 5.12, 5.13 and 5.14 without any viscosity change. The y-velocity propagates to the bottom due to the increasing external velocity until 5sec. After the velocity profile was fully developed, there were no changes any more.

ADINA

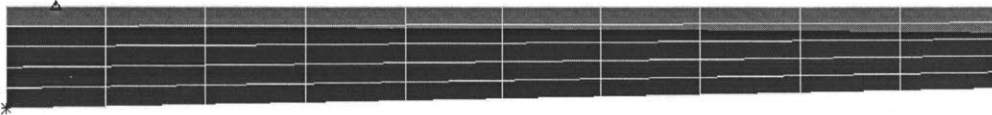


Y-VELOCITY
TIME 15.00



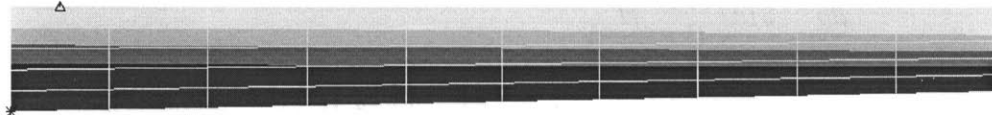
MAXIMUM
△ 0.002000
MINIMUM
* 0.000

TIME 1.000



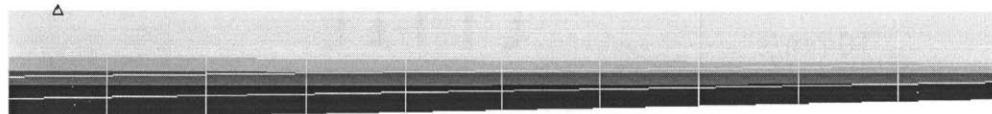
MAXIMUM
△ 0.004000
MINIMUM
* 0.000

TIME 2.000



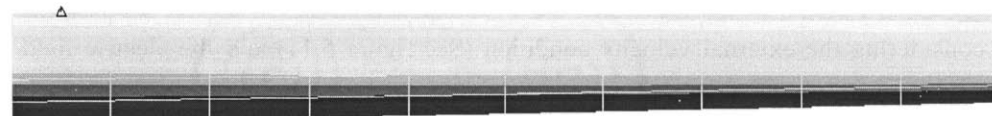
MAXIMUM
△ 0.006000
MINIMUM
* 0.000

TIME 3.000



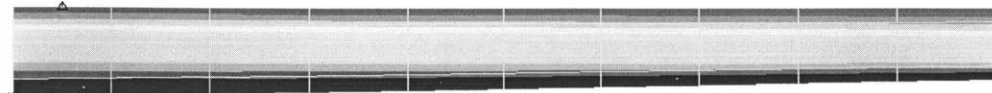
MAXIMUM
△ 0.008000
MINIMUM
* 0.000

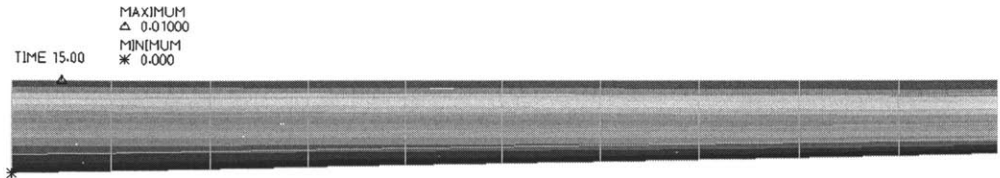
TIME 4.000



MAXIMUM
△ 0.01000
MINIMUM
* 0.000

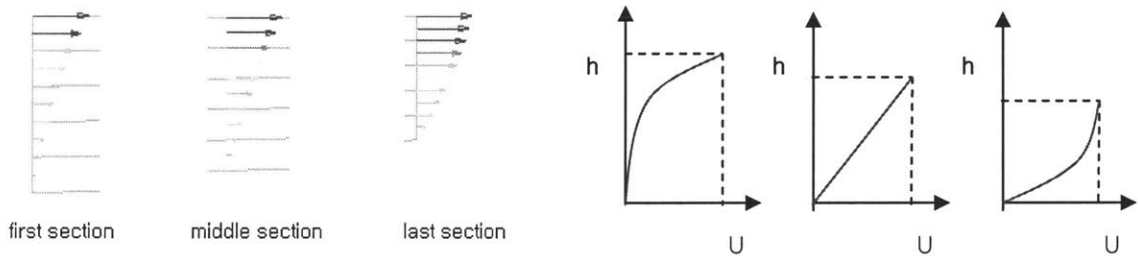
TIME 5.000





<Fig 5.12 - y- velocity profile in the inclined plate at 1,2,3,4,5 and 15 sec at 1kV/mm respectively : y-velocity propagates to the bottom until 5sec and after 5sec, the velocity profiles are same >

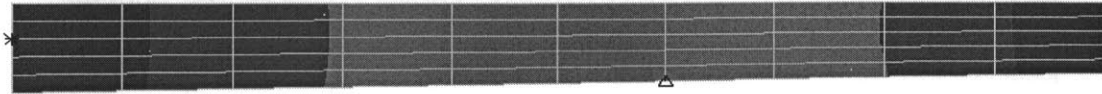
From formula (5.1), the velocity profile is not linear, because the pressure gradient existed due to inclined plates. To satisfy the mass conservation, the right side average velocity should be larger than that of the left side. After fully developed, the velocity vector was shown below and the mathematically expected velocity was also shown.



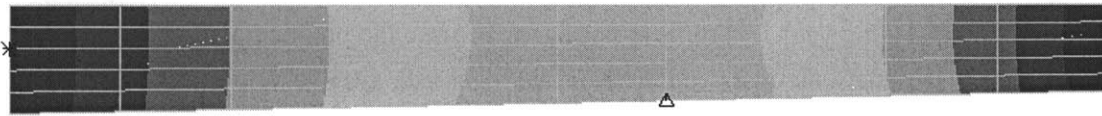
<Fig 5.13 –y- velocity profiles in the three sections : To satisfy continuity, the velocity profile is not linear anymore. Velocity profile is concave at the left side, and then it is linear at the middle section and then it is convex at the right side>



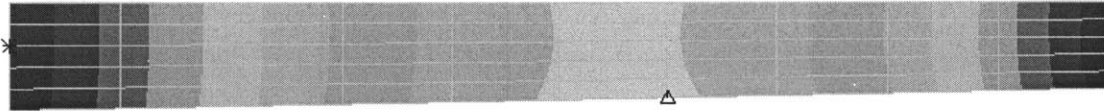
MAXIMUM
△ 10928.
MINIMUM
* 22.32 TIME 1.000



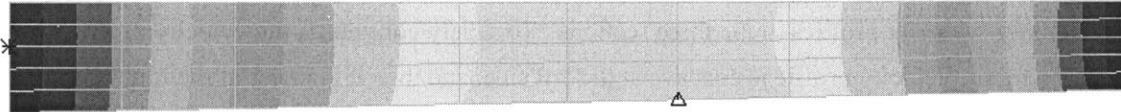
MAXIMUM
△ 21856.
MINIMUM
* 44.63 TIME 2.000



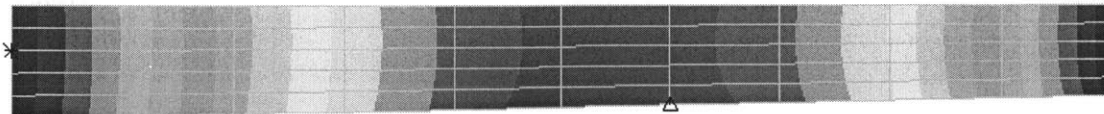
MAXIMUM
△ 32784.
MINIMUM
* 66.95 TIME 3.000



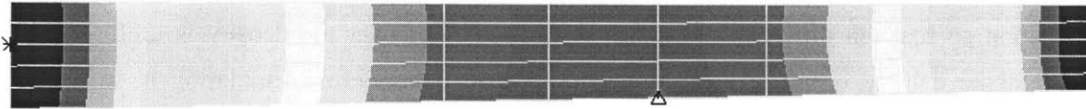
MAXIMUM
△ 43712.
MINIMUM
* 89.26 TIME 4.000



MAXIMUM
△ 54640.
MINIMUM
* 111.6 TIME 5.000

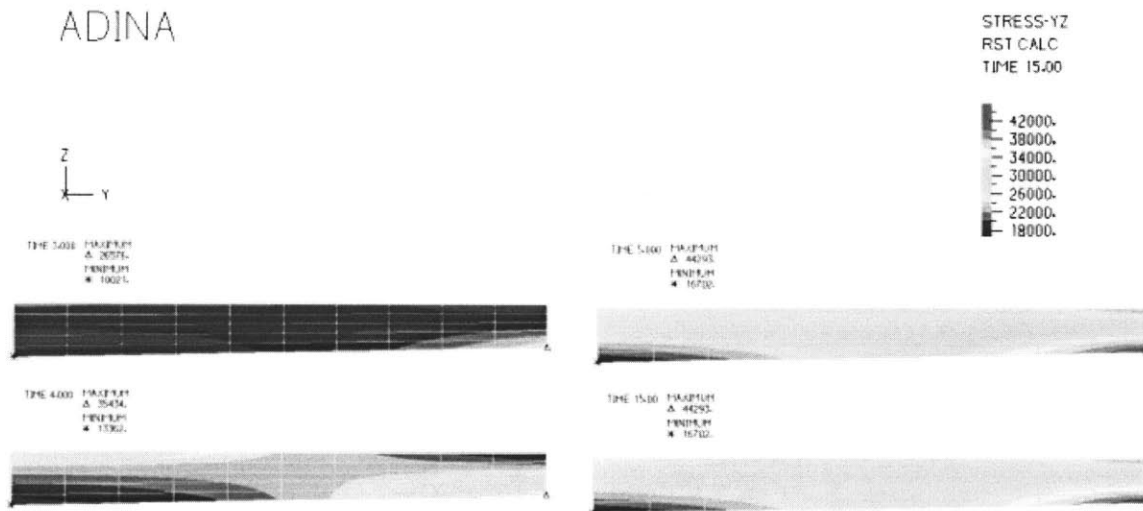


MAXIMUM
 Δ 54640.
 MINIMUM
 * 111.6 TIME 15.00



<Fig 5.14 – The pressure gradient when times are 1,2,3,4,5 and 15 sec at 1kV/mm:
 Due to the inclined plate, the pressure gradient was developed until 5sec>

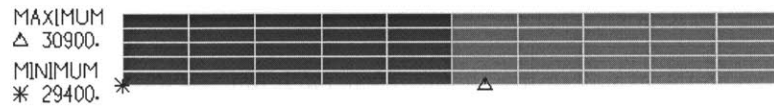
Shear stress is not uniform unlike the simple shear mode due to the inclined plates. To satisfy continuity, y-velocity profile is not linear, and. From figure 5.15, the shear stress has maximum value at the bottom of right side. As the figures 5.13 shows, the derivative value of the velocity profile is the largest at this point so that shear stress could be maximized.



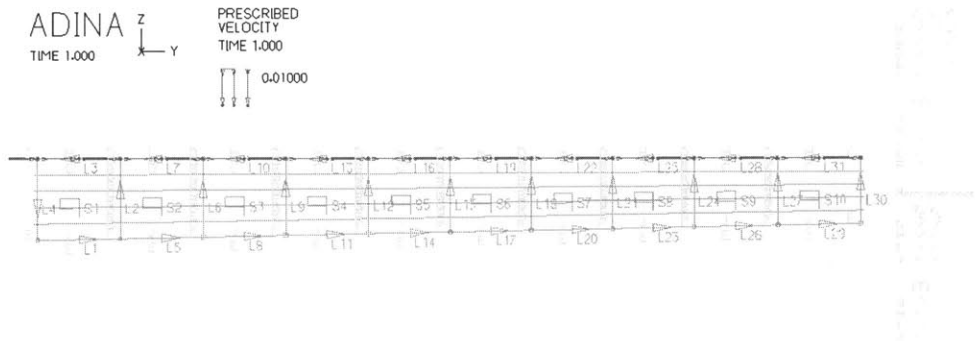
<Fig 5.15 – yz stress when times are 3, 4, 5 and 15 sec at 1kV/mm>

Considering homogeneous ER fluid whose viscosity was changed by the electric field strength, the viscosity should be changed at each section. Considered that the electric field of 2 (kV/mm) was applied to this structure and the electric field line is almost straight, the electric field strength along

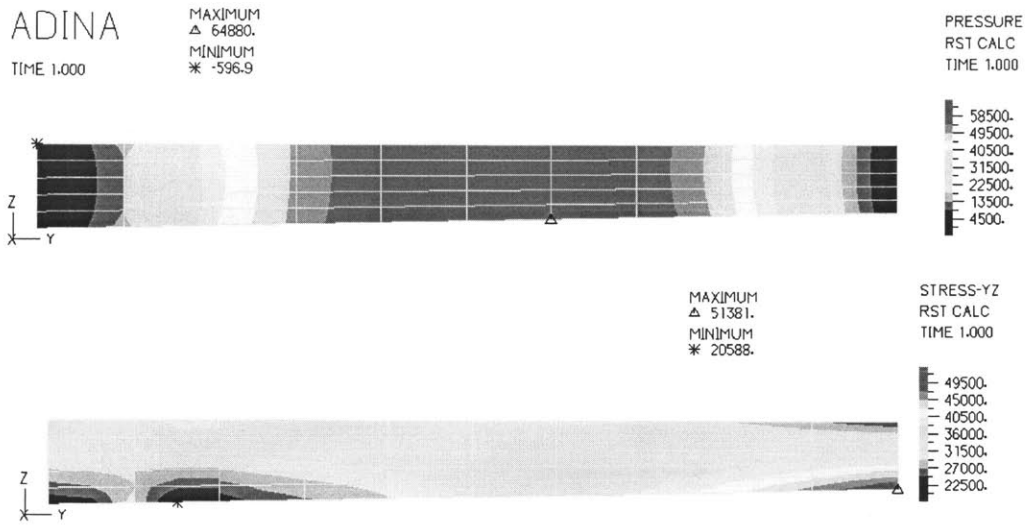
y-axis should be changed from 2(kV/mm) at the left side to 2.5 (kV/mm). Therefore, the viscosity should be changed from 29.4 (Pa ·s) to 30.9 (Pa ·s). For more simplification, it was assumed that the viscosity was changed linearly along the y-axis and each section has the same viscosity in the same section so that ten different viscosities were used. Moreover the density is uniform, i.e. it means that the density is not influenced by the electric field. Before simulating it, to check if viscosity could be changed, the simple shear mode at the rectangular geometry which has two different viscosities was tested. From the figure below, the shear stress was explicitly different at each region.



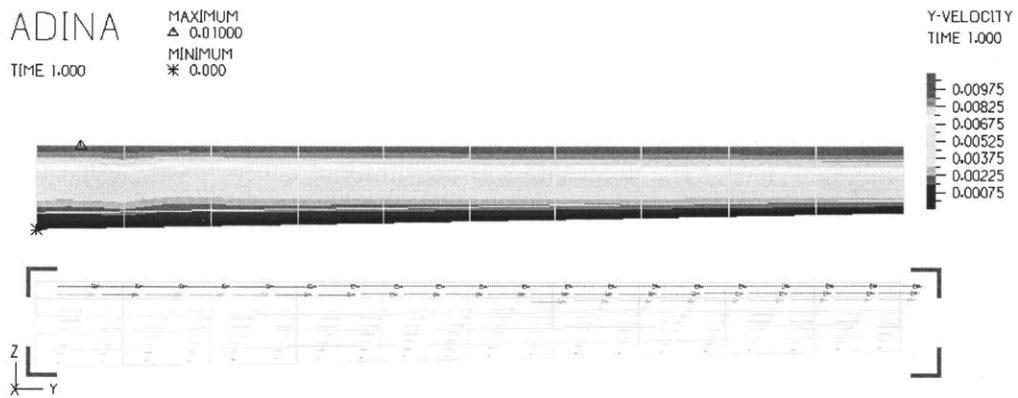
<Fig 5.16– shear stress when it has two different viscosities: 30.9 and 29.4 (Pa·s): the shear stress is different because of tow different viscosities >



<Fig 5.17 – The boundary conditions when the viscosities of elements are different: Each element has its own viscosity and 10 elements compose the whole structure >

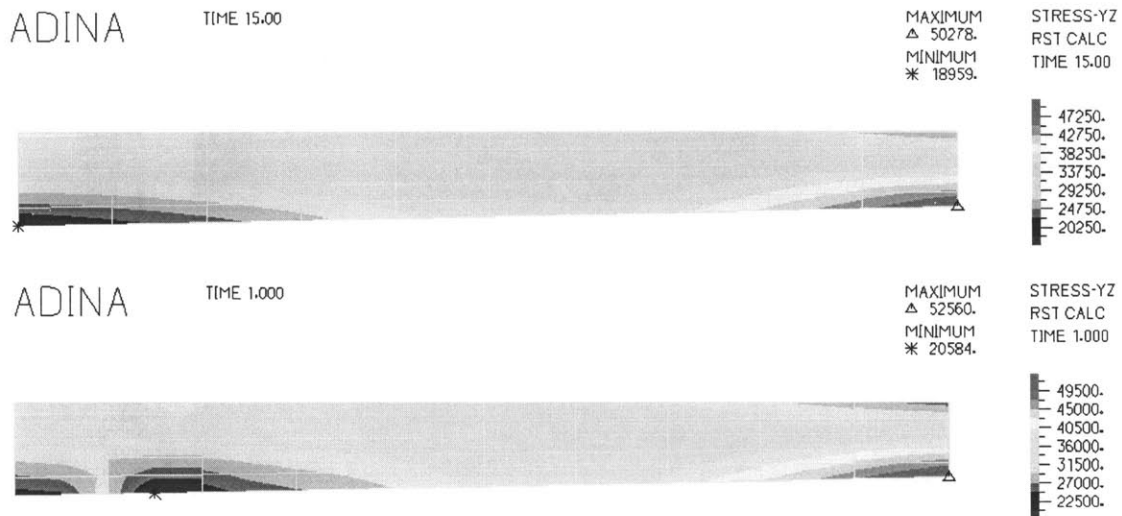


<Fig 5.18 – Pressure gradient and shear stress at 2kV/mm>



<Fig 5.19 – y-velocity distribution and profile at 2kV/mm >

From figure 5.17, the maximum shear stress larger than that of no viscosity change. Their difference between two maximum values is 2282 Pa (See figure 52560 Pa with varying viscosity – 50278 Pa with constant viscosity).



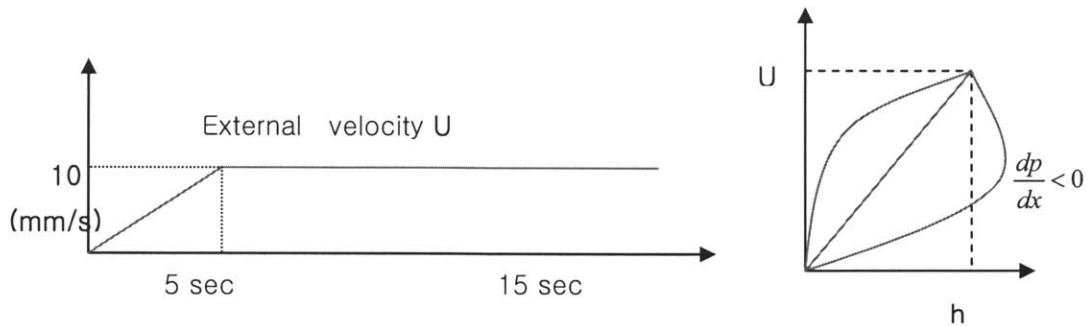
<Fig 5.20 – Shear stress at 2kV/mm when it has a constant viscosity and a variable viscosity >

Shear mode with the pressure gradient

When shear mode has the constant pressure gradient, the flow was developed by pressure and shear force. When the material was fully changed to fluid, the velocity profile was neither linear nor symmetric parabolic any more. The shear stress is not uniform, either. It was tested under the following condition. The external velocity was increased up to 10mm/s and then the velocity was kept steady. In addition to that, the electric field strength was assumed to be 2kV/mm, so that the viscosity of the homogenous ER fluid was 29.4 (Pa·s). Mathematically, the fluid velocity

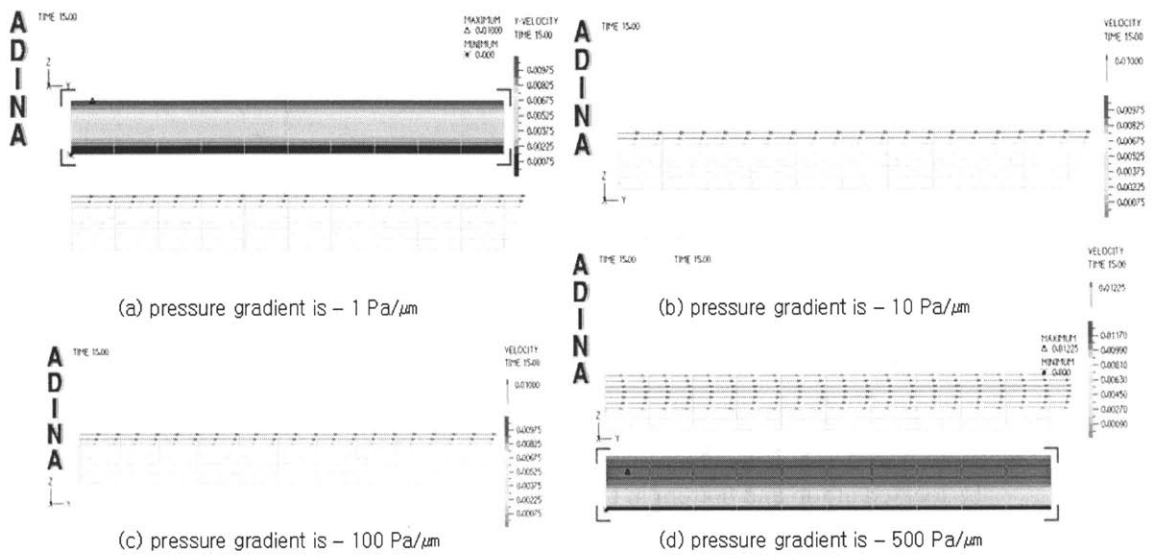
$$U(y) = \frac{1}{2\mu} \left(\frac{dp}{dx} \right) y^2 - \left(\frac{1}{2\mu} \left(\frac{dp}{dx} \right) h - \frac{U}{h} \right) y \quad \text{with} \quad \frac{dp}{dx} = \text{const}, \quad (5.3)$$

Therefore, if $\frac{dp}{dx}$ is negative, the velocity profile should be like the right graph of the figure 5.21

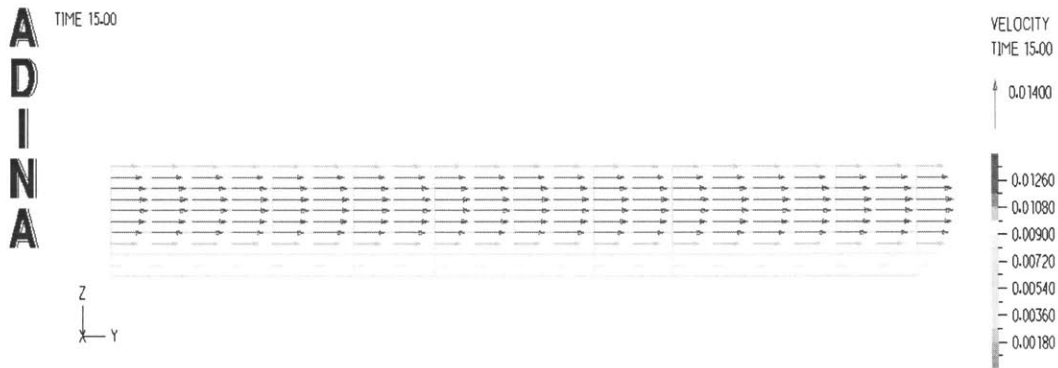


<Fig 5.21 – The external velocity condition for the shear mode with inclined plate and the flow velocity profile: the flow velocity is not linear due to the pressure gradient. When the pressure gradient is negative, max velocity exists inside the flow. On the other hand, max velocity would be located at top and bottom in the case of positive pressure gradient. >

Even though the pressure influence on the velocity existed explicitly, the influence by the pressure is so small that it can be ignored. The figure 5.22 showed how much the pressure gradient influenced on the velocity. When the pressure gradient was -1 (Pa/ μm) or 10 (Pa/ μm) or 100 (Pa/ μm), the influence by the pressure was so small that the maximum velocity was still at the top line due to the shear force. However, when the pressure gradient increases up to -500 (Pa/ μm), the maximum value of the velocity was located near the centerline and the value was 0.01125 (mm/s). At this case, the velocity profile was displayed as a asymmetric and quadratic form, while the other cases were almost linear. The viscosity of our homogeneous ER fluids is so large that the influence by pressure is not much as large as the heterogeneous case. In the case of heterogeneous ER fluid, its viscosity is smaller than that of the homogeneous ER fluid by $1/10$. Therefore, the pressure effect could not appear when the pressure gradient is smaller than 5000 (Pa/ μm). The figure 5.23 showed the y-velocity when heterogeneous ER fluid was fully fluid with the pressure gradient, -500 (Pa/ μm)



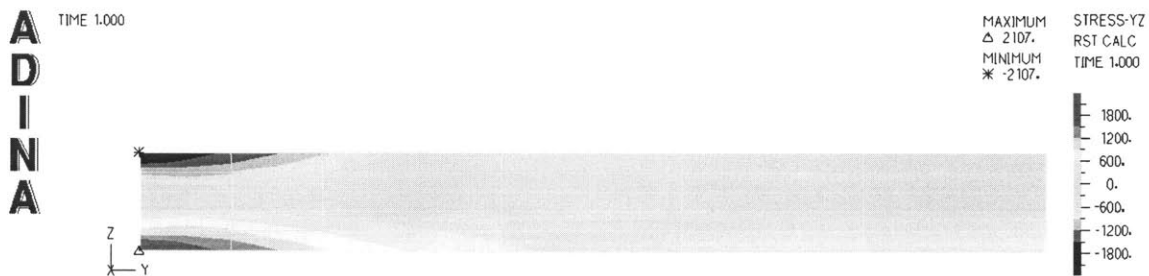
<Fig 5.22 – The velocity profiles at four different pressure gradients – the effect of pressure gradient could be observed when the pressure gradient is below $-500 \text{ (Pa}/\mu\text{m})$ >



<Fig 5.23 – The velocity profiles of heterogeneous ER fluid when pressure gradient is $-500 \text{ (Pa}/\mu\text{m})$: the velocity profile is neither linear nor symmetric due to pressure gradients >

Supposing that heterogeneous ER fluids is solid at $3\text{kV}/\text{mm}$, the shear stress by 12000 Pa is larger than the shear yield stress (2.4 kPa). Therefore, without any shear force, this material could be transitioned from solid to fluid. However, when the pressure is 10000 Pa , the shear stress by the pressure (2.1 kPa) was smaller than the shear yield stress (See figure 5.24). Therefore if we add the

shear force to the pressure by 300 Pa approximately, this material will start to flow from the upper part. Supposing that the pressure with 10000 Pa is applied, this material would remain solid throughout the region. Assuming that an additional shear force is applied to the material so that the left and upper part will start to flow and the solid area is decreased, the more shear stress at the top and bottom of solid region could be applied. For example, when the area of solid is decreasing by 10%, the shear stress increases by 3 times, which could make the solid region to transit to the fluid state faster. Therefore the whole region will be changed into fluid promptly.



<Fig 5.24 – Shear stress distribution when the pressure is 12000 Pa: the shear stress by the pressure (2.1 kPa) was smaller than the shear yield stress. Maximum shear stress is located at the top and bottom, so that those parts will start to flow first if an additional force is applied. >



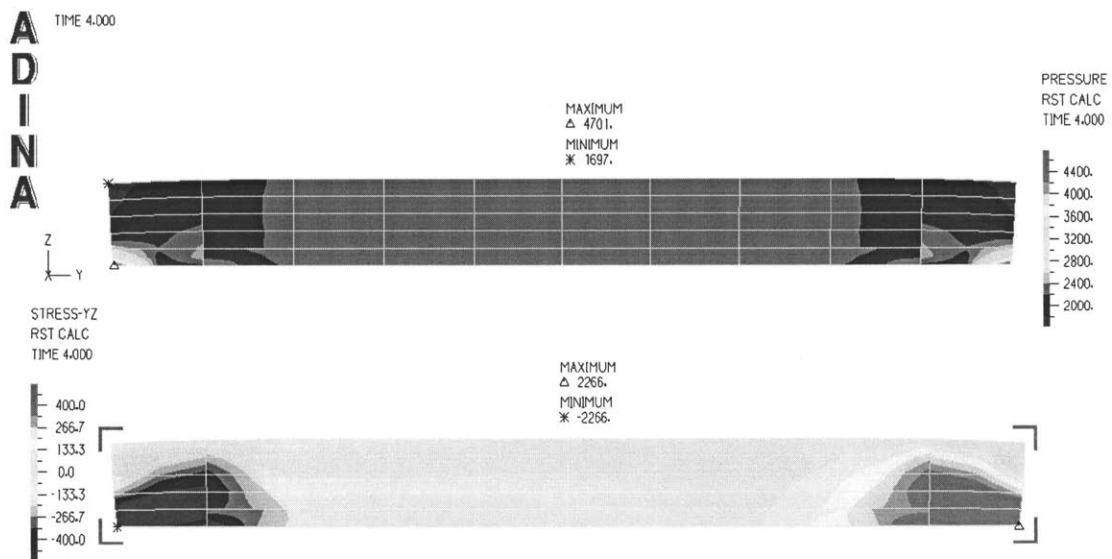
<Fig 5.25 – Shear stress distribution when the height is $9\mu\text{m}$: the maximum value is much larger than that of $10\mu\text{m}$ by 3 times so that the transition could finish faster >

Squeeze mode between two plates

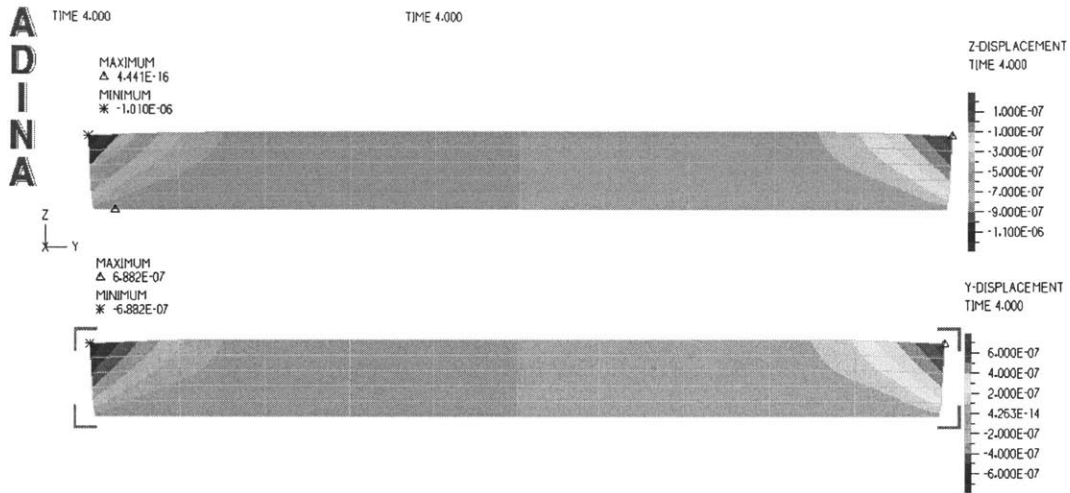
Squeeze mode was tested when the compression force (the pressure) is applied to the upper line. In case of solid, the displacement type of force or the pressure was applied. When the displacement

was increased by the external force, which is similar to the squeeze motion in case of the solid, the internal pressure and shear stress was increased.

When the pressure is applied to the upper line with the assumption that the pressure increment rate is 1000 (Pa/s), the shear stress distribution and pressure gradient was displayed as figure 5.26. From figure 5.26, when the displacement was almost $1\mu\text{m}$ at 4000Pa, the maximum shear stress was 2226 Pa which is almost same as the yield stress. Hence the over- value near 4000 Pa would be the critical pressure. Moreover the point to start the state transition would be the bottom at the both sides.

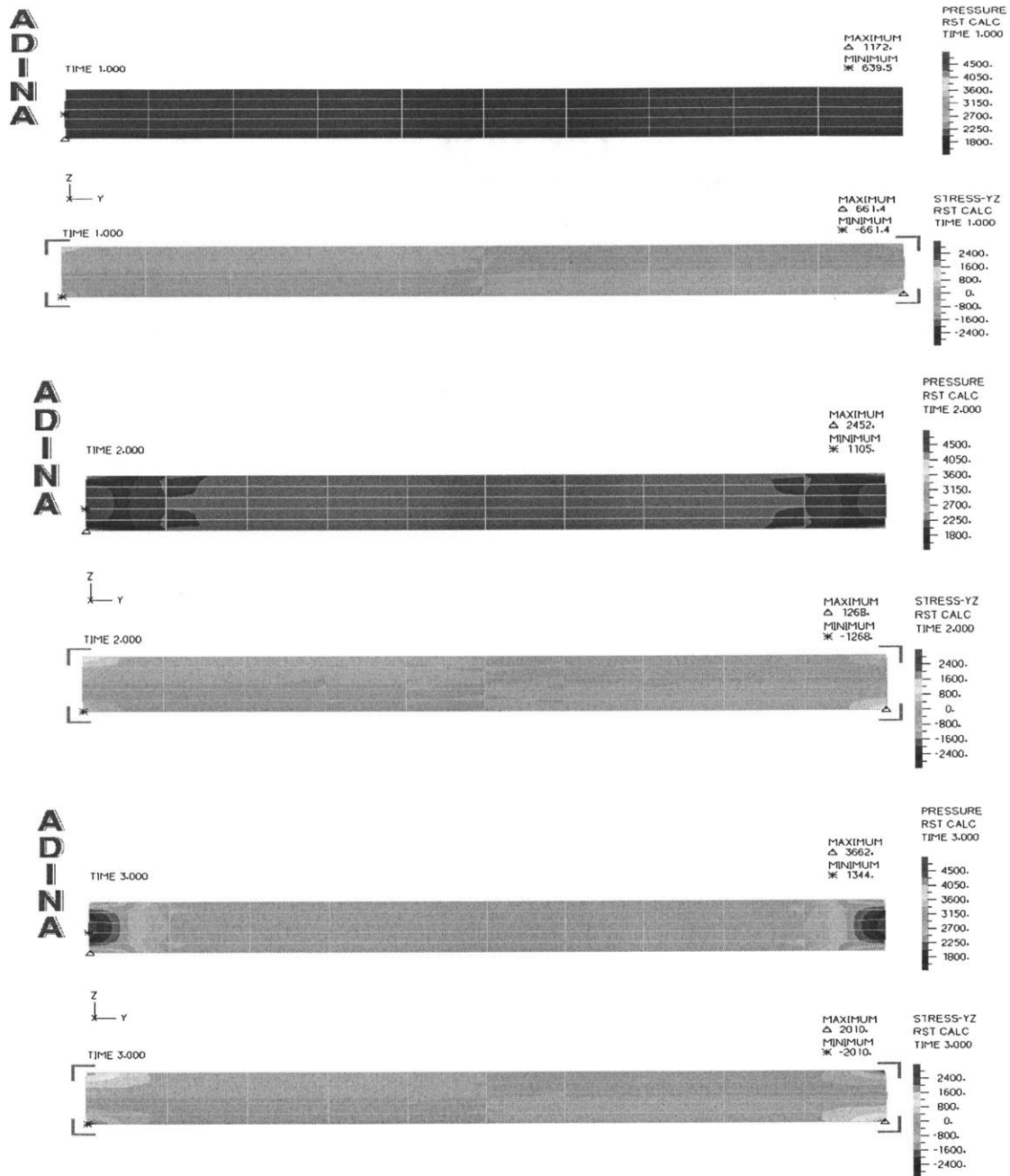


<Fig 5.26 – The pressure and shear stress distribution in the squeeze mode when the external pressure was increased by 1000Pa/s. the shear stress at bottom of both sides has maximum values and this value is near yield stress so that the critical pressure for the transition could be 4000Pa>

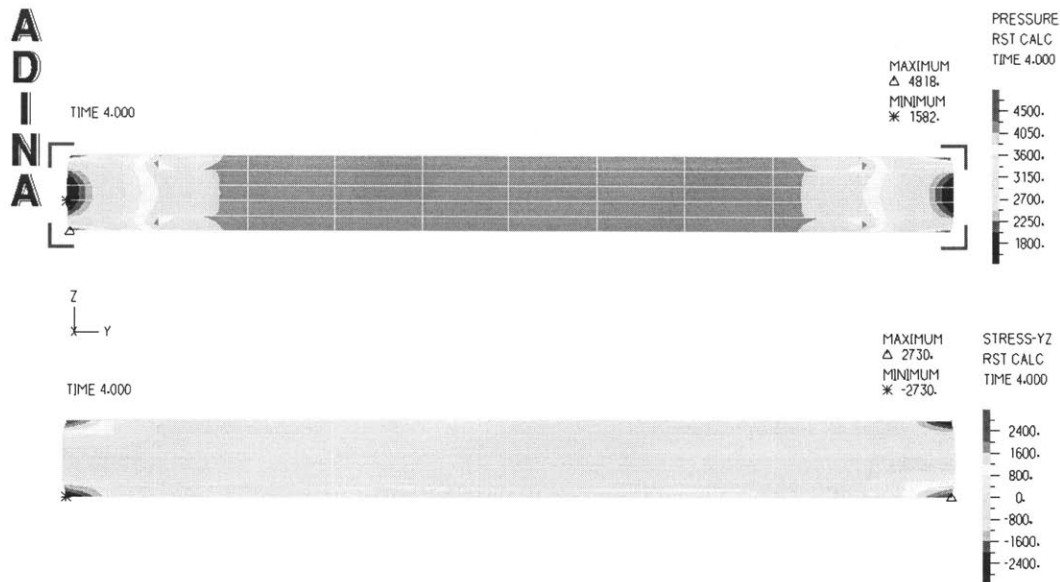


<Fig 5.27 – Y and z displacements when the pressure was 4000 Pa : Z-displacement is $1 \mu\text{m}$ when the shear stresses at the top and bottom of both sides are over shear yield stress. Y-displacement could be neglected, compared with the width >

Instead of the pressure, the change of displacement along z was tested when the velocity of the upper line was $0.25 \mu\text{m/s}$. when the z displacement was $-1 \mu\text{m}$, the shear stress was over the yield stress. (See figure 5.28) Hence, the results were similar to those by the pressure. The difference between two conditions, the maximum shear stress appeared at the bottom and top of both edges, because the upper line was displaced uniformly. In our case, the change of displacement could be much proper boundary condition. Considering the velocity profile of the fluid at both edges in the squeeze mode was almost symmetric and the continuity should be satisfied, the shear stress at the top and bottom of both edges should be same. Under either the compression of solid or the change of displacement of fluid, the material would start to transit at the both edges, and then this transition will be propagated to the center.

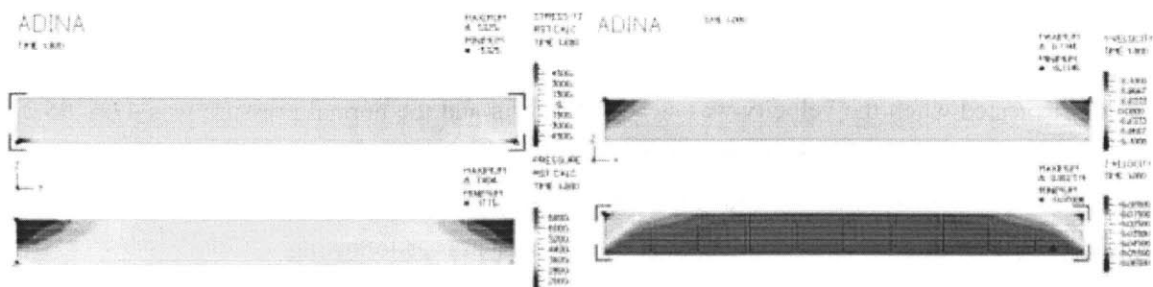


<Fig 5.28 – The internal pressure and shear stress distribution when the displacement was -0.25 , -0.5 , $-75(\mu\text{m})$: the pressure and shear stress are almost uniform except both sides. Maximum values of shear stress are located at the top and bottom of both sides so that the transition could start from those locations >

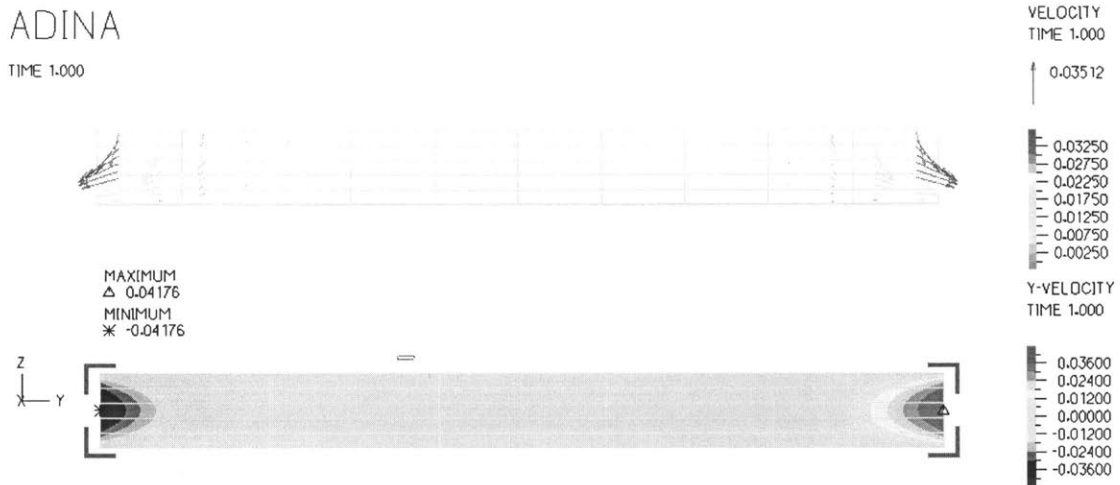


<Fig 5.29– The internal pressure and shear stress distribution when the displacement is $-1 (\mu\text{m})$: the shear stress is symmetric >

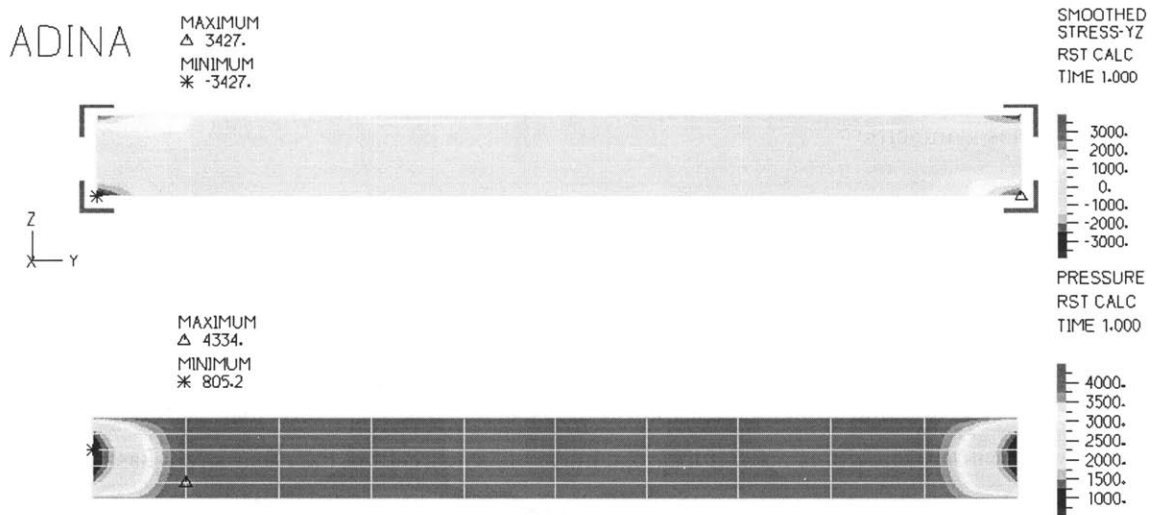
Assuming that the transition is so fast that the whole change could be completed when pressure is 4000Pa and the displacement change is $-1 (\mu\text{m})$ at same pressure, y-velocity profile and shear stress distribution at this time are as following (See figure 5.31 and figure 5.32). In this case, boundary conditions should be selected carefully. At the top, they can have z velocity, but might not have y-velocity because this line seems to be a wall. If they cannot have z-velocity, there is no effect on the velocity so that the velocity is zero. If they can move at any direction, the shear stress has maximum at the only bottom (See figure 5.30). However this case doesn't satisfy continuity because the top line should satisfy the no slip condition.



<Fig 5.30 – The velocity profiles and stress distribution under wrong boundary conditions>



<Fig 5.31 – The velocity profile and y-velocity distribution at transient state under 4000 Pa>



<Fig 5.32 – The shear stress and pressure distribution at transient state under 4000 Pa>

Shear mode with the normal force

It was tested when the velocity was steady at 8mm/s and the normal pressure was 47.6, 95.2 and 190.4(Pa) respectively. It seems to be the mixed with the shear mode and the squeeze mode. In this case, the normal force is not enough to influence on the deformation of the structure. From the simple calculation, the maximum value of z displacement is as following:

$$\Delta l = \tau \cdot \frac{l}{E} \quad (E \text{ is Young's modulus}) \approx \frac{10(\mu m)}{20.80(kPa)} \cdot 200 \approx 10^{-7} \quad (5.4)$$

This change of displacement has little effect on the shear stress increment, so that that it can be neglected.

5.2 Conclusion

So far, some simulations under the basic three operating modes were tested in the case of Bingham plastic fluid (Heterogeneous ER fluid) and Newtonian fluid (Homogeneous ER fluid).

In shear mode, both materials were simulated with the following boundary conditions: both side lines were symmetric for the infinite condition. The top line was moving and the bottom line was fixed. The results showed the characteristic of both fluids.

In pressure mode, the behavior of the homogeneous ER fluid followed the mathematical modeling. In the mixed condition of pressure and shear modes, it also mimicked the similar behavior, compared with the mathematical calculations. Heterogeneous fluids with FEM presented some challenges. Because ADINA doesn't support a multi-physical state between a solid and a fluid, only the starting point or critical point of the transition state could be predicted using a plastic bilinear model.

In squeeze mode, the boundary conditions were important in order to simulate how the upper line could transfer force to the fluid. When pressure was applied, the result couldn't be consistent with the no-slip condition of the fluid. When the condition of displacement change was applied, the result has consistency.

Other cases such as variable viscosity or shear mode with a small normal force were tested and their influence on the shear mode was so small that they could be neglected.

5.3 Future work

Since the invention of ER fluids, they have been investigated with focus on material properties and the behavior mechanisms of ER materials. In addition, the number of application using ER material has increased. Nevertheless, the commercial applications have not been pursued as much as

basic testing. Therefore we need to investigate their availability or controllability more. For this reason and the project's long term goal, further investigations or other approaches to the ER materials need to be performed.

Above all, other operating modes such as bending mode and impulsive loading mode need to be tested. Also, more complex structures and geometries such as two or three layered structure also need to be investigated.

Secondly, unlike the other basic modes, the mathematical modeling of the squeezing mode could not be fully completed, because Bingham plastic properties was not suitable this mode. Hence, a proper mathematical model should be developed. ER fluids could be considered one of the viscoelastic materials from many articles. Their storage modulus and loss modulus have been measured by many researchers. And its parametric models have been suggested [41]. Hence, as an alternative approaches, a viscoelastic model also should be developed. Moreover, the more fitted mathematical modeling for this mode needs to be investigated.

Thirdly, the FEM model did not describe the transient state well. In reality, some parts could remain solid, while other parts change into fluid at specific locations and conditions. However, ADINA cannot simulate the multiple states between a solid and a fluid. Other FEM software (commercial or user-programmed) for Bingham plastic fluids need to be developed. In addition, new developed ER fluid which has much larger shear yield stress than any other developed ER fluids should be investigated for our long term purpose.

Bibliography

- [1] T. Hao. Electrorheological fluids. *Advanced Material*, 13(24):1847-1857, 2001
- [2] T. C. Halsey. Electrorheological fluids. *Science*, 258(30):761-766, October 1992
- [3] J.Park and O. Park. Electrorheology and magnetorheology. *Korea-Australia Rheology Journal*,13(1):13-17, March 2001 pp.
- [4] T. C. Jordan and M. T. Shaw, "Electrorheology", *IEEE Transactions on Electric Insulation*, 24(5):849-878, 1989.
- [5] A.V.Srinivasan and D.Michael Mcfarland. *Smart structures: Analysis and Design*, Cambridge University Press, 2001
- [6] P. J. Rankin, J. M. Ginder and D. J. Klingenberg. Electro- and magneto-rheology. *Current Opinion in Colloid & Interface Science*, 3:373-381, 1998
- [7] M. Parthasarathy and D. J. Klingenberg. Electrorheology: mechanisms and models. *Materials Science and Engineering*, R17:57-103, 1996
- [8] W. Wen, X. Huang, S. Yang, J. Lu and P. Sheng. The Gigantic electrorheological effect in suspensions of nanoparticles. *Nature Materials*, 2:727-730, November 2003
- [9] H. Conrad, A.F. Sprecher, Y. Choi and Y. Chen. The temperature dependence of the electrical properties and strength of electrorheological fluids. *Journal of Rheology* 35(7):1393-1410, October 1991
- [10] B.Engelmann, R.Hoptmair, R.H.W Hoppe and G.Mazurkevitch. Numerical simulation of electrorheological fluids based on an extended Bingham model. *Sonderforschungsbereich 438*, March 1999
- [11] W. Torr. Structural formation in electrorheological fluids. *Journal of Colloid & Interface Science*, 156:335-349, 1993
- [12] K. Sekimoto. Motion of the yield surface in a Bingham fluid with a simple-shear flow geometry. *Journal of Non-Newtonian Fluid Mechanics*, 46:219-227, 1993
- [13] Y. Otsubo and K. Edamura. Static yield stress of electrorheological fluids. *Journal of Colloid & Interface Science*, 172:530-535, 1995
- [14] T. Hao, A. Kawai and F.Ikazaki. The yield equation for the electrorheological fluids. *Langmuir*, 16:3058-3066, 2000

- [15] A. Inoue, U. Ryu and S. Nishimura. Caster-walker with intelligent brakes employing ER fluid composed of liquid crystalline polysiloxane. Proceedings of the Eighth International Conference: 23-29, 2001
- [16] A. Inoue, Y. Ide, S. Maniwa, H. Yamada and H. Oda. ER fluids based on liquid crystalline polymers, MRS Bulletin: 43-49, August 1988
- [17] Going with the flow. Economist, Technology Quarterly <http://www.economist.com/science/tq/displayStory.cfm?story_id=2724363>
- [18] D. K. Cheng. Field and wave electromagnetics, 2nd edition. Addison-Wesley Publishing Company, Inc, 1989
- [19] K. Bathe. Finite element procedure. Prentice-Hall, Inc. 1996
- [20] D. Cartling and N. Phan-thien. A numerical simulation of a plastic fluid in a parallel-plate plastomer. Journal of Non-Newtonian Fluid Mechanics, 14:347-360, 1984
- [21] M. R. Jolly, J. W. Bender and J. David Carlson. Properties and applications of commercial magnetorheological fluids. SPIE--The International Society for Optical Engineering, 3327:262-275, 2003
- [22] Lord Materials Division, "What is the Difference between MR and ER Fluid" Presentation, May 2002.
- [23] A. Hosseini-Sianaki, C. J. Varley, P. M. Taylor, C. Malins and D. Lacey. Comparison of ER fluids based on Silicone oil and liquid crystalline materials. Journal of Material Chemistry, 5(11): 1853-1856, 1995
- [24] C. Malins and D. Lacey. Evaluation of ER fluids incorporating liquid-crystalline materials. Journal of Material Chemistry. 4(7): 1029-1033, 1994
- [25] D. Lacey and C. Malins/P.M. Yaylor, A. Hosseini-sianaki and C.J. Varley. Investigation into the use of liquid crystal materials in electrorheological fluids. Journal of Intelligent material systems and structures. 7 September 1996
- [26] N. Yao and A.M. Jamieson. Electrorheological behavior of side-chain liquid-crystalline polysiloxanes in nematic solvents. Macromolecules 30:5822-5831, 1997
- [27] K.H. Huebner, E.A. Thornton, The Finite Element Method for Engineers, Second Edition, John Wiley and Sons, 1982.
- [28] Hughes, T. J. R., 1987, The Finite Element Method. Linear Static and Dynamic Finite Element Analysis, Prentice-Hall, Inc.
- [29] S. Choi, S. Hong and H. Song, The applications of the smart ER fluids, Korean machine and materials, 14(4):35-48, 2002

- [30] S. Morishita and J. Mitsui. An electronically controlled engine mount using ER fluid. SAE technical paper series 922290, 1992
- [31] S. Drakunov, U. Ozguner, P. Dix and B. Ashrafi. ABS control using optimum search via sliding modes. IEEE Transaction on Control Systems Technology. 3(1) :79-85, 1995
- [33] Y.Akagami, S. Nishimura and Y.Ogasawara. Polishing of microholes using ER fluid under alternative electric field. Proceedings of the 6th international conference on ER fluids: 803-808, 1997
- [34] Y.Akagami, K. Asari, B. Jeyadevan, T. Fujita and N. Umehara. ER fluid finishing using rotating electrode. Proceedings of the 7th international conference on ER fluids: 821-826, 1999
- [35] J.P.Coulter, P. Keith, D.Weiss and J. D. Carlson. Engineering applications of electrorheological materials. Journal of Intelligent Material Systems and Structures 4:248-259, 1993
- [36] J.L. Sproston, S.G. Rigby, E.W.Williams and R.Stanway. A numerical simulations of electrorheological fluids in oscillatory compressive squeeze flow. Journal of Physics D :Applied Physics. 27:338-343, 1994
- [37] V.Noresson,N.-G. Ohlson. A critical study of the Bingham model in squeeze-flow mode. Materials and Design 22:651-658, 2001
- [38] D.K. Gartling and N. Phan-thien. A numerical simulations of a plastic fluid in a parallel plate plastomer. Journal of Non-Newtonian Fluid Mechanics, 14:347-360, 1984
- [39] A. Lawal and D.M. Kalyon. Squeezing flow of viscoplastic fluids subject to wall slip. Polymer engineering and science. 38(11):1793-1804, 1998
- [40] F. Yang. Exact solution for compressive flow of viscoplastic fluids under perfect slip wall boundary conditions. Rheological Acta. 37:68-72, 1998
- [41] T. Butz O. von Stryk. Modeling and Simulation of ER and MR Fluid Dampers. ZAMM. 82(1):3-20, 2002
- [42] D.R.Gamota, F.E.Filisko. Dynamic mechanical studies of electrorheological materials: Moderate frequencies. Journal of Rheology. 35:399—425, 1991
- [43] B. F. Spencer jr., S. J.Dyke, M. K. Sain, J. D. Carlson. Phenomenological model of a magnetorheological damper. Journal of. Engineering Mechanics. Mech. 123:230-238,1997
- [44] M.Nilsson and N.G.Ohlhson. An ER Fluid in Squeeze mode. Journal of Intelligent Material Systems and Structures. 11:545-554, 2000
- [45] H. Conrad. ER fluids: characteristics, structure and mechanisms. ASME Electro-Rheological Flows 164:99-113, 1993

- [46] M. Whittle. Computer simulations of an ER fluid. *Journal of Non-Newtonian fluid mechanics*, 37:233-263, 1990
- [47] Y. Zhao, T. Xiao, J. Zhao. The modeling of layered plates featuring electro-rheological material layer and its numerical and experimental validations. *Aerospace Science and Technology* 6:53–62, 2002
- [48] D. Kim, Numerical Computations for incompressible Navier-Stokes equations using finite element method
- [49] Finite Element Method. Computer Simulation in Acoustics at University of Salford. http://www.acoustics.salford.ac.uk/student_area/bsc3/computer_simulation/Fem.pdf
- [50] Huebner K.H., Thornton E.A., *The Finite Element Method for Engineers*, Second Edition, John Wiley and Sons, 1982
- [51] F. A. Morrison. *Understanding Rheology*, Oxford University Press, 2001
- [52] A. Cebers, E. Lemaire, L. lobry. Flow modification induced by Quincke rotation in a capillary. *International Journal of Modern Physics B [Condensed Matter Physics; Statistical Physics; Applied Physics]*, 16(17-18):2603-2609, 2002
- [53] D.E. Eastman IV. Design of semi-active variable impedance materials using field-responsive fluids. Master thesis, MIT, June 2004